

Quantumness of gravity in harmonically trapped particles

Youka Kaku,^{1,*} Shin'ya Maeda,^{1,†} Yasusada Nambu,^{1,‡} and Yuki Osawa^{1,§}

¹*Department of Physics, Graduate School of Science,
Nagoya University, Chikusa, Nagoya 464-8602, Japan*

(Dated: December 10, 2022)

This study investigates the quantumness of gravity under the setup of the atomic interferometry from the viewpoint of mass-energy equivalence. We evaluated interference visibility considering a particle with internal energy levels in a harmonic trapping potential. As per the result, for a spatially superposed gravitational source mass, interference visibility exhibits collapse and revival behavior, which implies that an initial separable internal state evolves to the entangled state with respect to the degrees of freedom of the center of mass, the internal energy levels, and the external source state. In particular, it does not exhibit revival behavior when gravity is treated as a quantum interaction, while it revives with a finite period for a semiclassical treatment of gravity. We also examined the temporal behavior of entanglement negativity and found that the nonrevival behavior of visibility reflects the creation of the entanglement between the internal energy state and the external source state which is uniquely induced by the quantum interaction of gravity in accordance with the weak equivalence principle.

I. INTRODUCTION

The unification of gravity and quantum theory is one of the most challenging subjects in modern physics because the experiment to test quantum gravity has not been realized thus far. Nevertheless, there are several experiments that focus on the quantum aspect of a particle under the classical external gravitational field to examine the relation between quantum mechanics and classical gravity [1]. For example, in the Colella-Overhauser-Werner (COW) experiment [2], the difference in gravitational potential causes the phase difference of a quantum particle and leads to gravity-induced quantum interference. This phenomenon was confirmed in the experiment using a neutron interferometer [3].

As a further development of quantum experiments under classical gravity, the authors of paper [4] discuss the decoherence mechanism of a quantum particle with internal (INT) degrees of freedom using mass-energy equivalence. Herein, the particle with the INT degrees of freedom is characterized by two systems: center of mass (CM) system and INT system. According to mass-energy equivalence, the particle acquires a different mass depending on the INT energy levels. Therefore, the dynamical variables of the CM and the INT systems entangle via special relativistic and gravitational couplings, which is known as universal gravitational decoherence. As a result, when atomic interferometry is considered, the interference visibility of the INT state exhibits collapse and revival behavior. Although time dilation due to classical gravity in a quantum clock system is recently measured in a feasible laboratory experiment [5], universal gravitational decoherence has not been confirmed yet. In addition, details regarding the entanglement behavior have been studied in [6, 7], and the gravitational decoherence in the Ramsey interferometry is also discussed by Haustein *et al.* [8].

Although the COW experiment [2] and the gravitational decoherence introduced by Pikovski *et al.* [4] treat the quantum system under classical external gravity, they focus on the quantum aspects of the probe particle rather than the quantumness of gravity. Recently, as the first step to tackle the quantumness of gravity, ideas based on quantum information have been proposed to test the quantumness of low-energy Newtonian gravity in tabletop experiments. These ideas are referred to as the Bose-Marletto-Vedral (BMV) proposal [9–11], and are based on the principle of quantum information theory, which states that local operations and classical communication (LOCC) cannot create entanglement between two systems [12]. Based on this principle, gravity can be clarified as a quantum interaction or not by detecting the creation of gravity-induced entanglement. The BMV proposal received a lot of attention, and has stimulated many other related proposals [13–15]. In interferometry experiments, the creation of entanglement between the probe and the environment is reflected in the quantum decoherence of the probe system [16–18]. Carney *et al.* [19] explored the quantum gravity-induced decoherence in a hybrid system that comprised a massive oscillator and a source mass particle in cat state, while some comments on this paper are discussed in [20] that LOCC with stochastic noise in the system can also reproduce the decoherence.

* kaku.yuka.g4@s.mail.nagoya-u.ac.jp

† maeda.shinya.k2@s.mail.nagoya-u.ac.jp

‡ nambu@gravity.phys.nagoya-u.ac.jp

§ osawa.yuki.e8@s.mail.nagoya-u.ac.jp

We note here that the purpose of the BMV proposal and other related proposals is to confirm if gravity produces quantum entanglement in the nonrelativistic scale. These proposals just assume that the Newtonian gravitational potential is treated as a two-body operator between gravitational sources, which is the consequence of the quantum field theory to explain the gravitational force by exchanging gravitons. Even though gravity-induced entanglement does not lead to the quantization of the gravitational field immediately, it is worth a try to explore as the first step to investigating quantum gravity for the following two reasons; First, it may be possible to detect gravity-induced entanglement in the near future as another way to approach the quantum feature of gravity based on the recent progress in the quantum experiments of macroscopic objects. For instance, since we need to treat the Planck energy scale under strong gravity, such as nearby the blackhole, to detect graviton, it is challenging to obtain direct evidence of graviton with terrestrial colliders. On the other hand, gravity-induced entanglement is expected to be the new direction to confirm the quantumness of gravity by focusing on the gravity of the Planck mass object in the tabletop experiment, although it cannot support the existence of graviton directly. Second, testing the gravity-induced entanglement in the nonrelativistic scale gives a valuable clue to the Newtonian limit of quantum gravity. Respecting the above, we will investigate gravity-induced quantum entanglement, which we refer to as the quantumness of gravity throughout this paper.

In this study, we propose a new approach to capture the quantumness of gravity in the Ramsey interferometry from the point of view of mass-energy equivalence. We assumed that a probe particle with two energy levels as the INT degrees of freedom is trapped in the harmonic oscillator potential, and feels external gravity, which mass source is in a cat state. Based on this setup, we aim to detect the interference visibility of the probe particle in Ramsey interferometry and calculate it for two cases; when the external gravity produces the entanglement between the probe particle system and the gravitational mass source system, or not. To perform a specific calculation, we adopt a particular form of gravitational interaction. For the former case, we assume the first quantization of Newtonian gravity in Eq. (17), which contains operators of both the particle and the source system and produces quantum entanglement between them. For the latter case, we assume the semiclassical gravity[21–23] which will be introduced in Eq. (22). Herein, semiclassical means that the gravitational mass source is quantized, but gravity remains fundamentally classical. As a result, we will show that the quantumness of gravity is reflected as a nonrevival behavior of the interference visibility, and that it is related to the creation of genuine tripartite system entanglement. We will also see that under the leading order approximation with respect to the separation of the source, this nonrevival behavior does not appear for other quantum interactions such as the electromagnetic Coulomb interaction respecting the weak equivalence principle; Our proposal successfully captures quantum nature unique to gravity.

The structure of the remainder of this paper is as follows. In Sec. II, we will briefly review the Ramsey interference [24]. In Sec. III, we explore a particle with INT degrees of freedom in an external gravitational field. In Sec. IV we introduce the experimental setup, calculate the transition probability in Ramsey interference following Haustein *et al.* [8], and reveal the behavior of the interference visibility under quantum superposition of gravitational source. In Sec. V, we estimate the creation of entanglement by calculating the entanglement negativity. Section VI, we discuss the results of the study and explore the comparison of quantized gravity and other quantum interactions. Section VII presents a summary of this study. The unit of $\hbar = 1$ was adopted throughout the study.

II. RAMSEY INTERFEROMETRY

In this section, we briefly review the concept of Ramsey interferometry [24–26]. Considering a particle (atom) with two internal energy levels, the Hamiltonian of the particle can be expressed as

$$\hat{H} = \sum_{j=0,1} \hat{H}_j |E_j\rangle \langle E_j|, \quad \langle E_j | E_k \rangle = \delta_{jk}, \quad (1)$$

where $|E_j\rangle$ denotes the j th internal energy eigenstate, and \hat{H}_j denotes the CM Hamiltonian of the particle associated with the j th internal energy level. The evolution operator of the total state is expressed as

$$\hat{U}(t) = \exp[-i\hat{H}t] = \sum_j \hat{U}_j(t) |E_j\rangle \langle E_j|, \quad (2)$$

where $\hat{U}_j = \exp(-i\hat{H}_j t)$ is the evolution operator of the particle state with the j th internal energy level. The Ramsey interferometry is performed as per the following steps (Fig. 1):

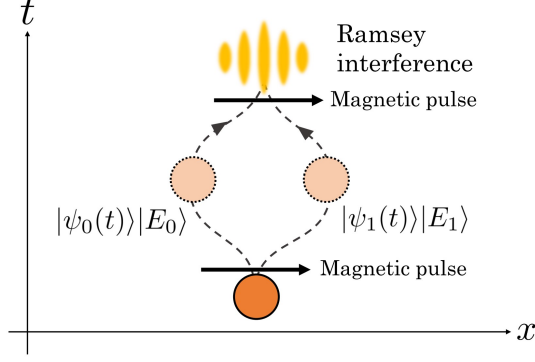


FIG. 1. Schematic representation of Ramsey interferometry using a superposed particle with different internal energy levels. After evolution, information on the INT state is obtained from the interference visibility.

Step 0: Prepare the initial state of the particle with the internal energy E_0 :

$$|\Psi(0)\rangle = |\psi(0)\rangle \otimes |E_0\rangle, \quad (3)$$

where $|\psi(0)\rangle$ denotes the initial CM state.

Step 1: Apply a $\pi/2$ -pulse to take the initial state into a superposition of two internal energy eigenstates:¹

$$|\Psi'(0)\rangle = |\psi(0)\rangle \otimes (|E_0\rangle + |E_1\rangle) / \sqrt{2}. \quad (4)$$

Step 2: Evolve the superposed state $|\Psi'(0)\rangle$ with the evolution operator mentioned in Eq. (2) up to time t :

$$|\Psi(t)\rangle = \hat{U}(t) |\Psi'(0)\rangle = \left(\hat{U}_0(t) |\psi(0)\rangle \otimes |E_0\rangle + \hat{U}_1(t) |\psi(0)\rangle \otimes |E_1\rangle \right) / \sqrt{2}. \quad (5)$$

Step 3: Apply the $\pi/2$ -pulse again to make the INT state as $|E_0\rangle \rightarrow (|E_0\rangle + |E_1\rangle) / \sqrt{2}$, $|E_1\rangle \rightarrow (|E_0\rangle - |E_1\rangle) / \sqrt{2}$:

$$\begin{aligned} |\Psi'(t)\rangle &= \frac{1}{2} \left[\hat{U}_0(t) |\psi(0)\rangle \otimes (|E_0\rangle + |E_1\rangle) + \hat{U}_1(t) |\psi(0)\rangle \otimes (|E_0\rangle - |E_1\rangle) \right] \\ &= \frac{1}{2} \left[\left(\hat{U}_0(t) + \hat{U}_1(t) \right) |\psi(0)\rangle \otimes |E_0\rangle + \left(\hat{U}_0(t) - \hat{U}_1(t) \right) |\psi(0)\rangle \otimes |E_1\rangle \right]. \end{aligned} \quad (6)$$

Step 4: Measure the occupation probability of the lower energy eigenstate $|E_0\rangle$:

$$\begin{aligned} P(t) &= \frac{1}{4} \langle \psi(0) | (\hat{U}_0^\dagger + \hat{U}_1^\dagger) (\hat{U}_0 + \hat{U}_1) | \psi(0) \rangle \\ &= \frac{1}{2} \left(1 + \text{Re} \left[\langle \psi(0) | \hat{U}_0^\dagger(t) \hat{U}_1(t) | \psi(0) \rangle \right] \right) \\ &= \frac{1}{2} \left(1 + \text{Re} \left[\langle \psi_0(t) | \psi_1(t) \rangle \right] \right). \end{aligned} \quad (7)$$

Herein, $|\psi_i(t)\rangle \equiv \hat{U}_i |\psi(0)\rangle$. Expressing $\langle \psi_0(t) | \psi_1(t) \rangle = |\mathcal{V}(t)| e^{i\Theta(t)}$ with real functions $|\mathcal{V}|$ and Θ , the occupation probability is expressed as

$$P(t) = \frac{1}{2} (1 + |\mathcal{V}(t)| \cos \Theta(t)). \quad (8)$$

Herein, $|\mathcal{V}(t)|$ is the interference visibility, which contains information regarding the internal energy levels of the particle. For example, if $H_i = E_i$, then $\hat{U}_j(t) = e^{-iE_j t}$ and $P(t) = \frac{1}{2} (1 + \cos(\Delta E t))$, $\Delta E = E_1 - E_0$. By measuring this probability as the function of time, we can determine an energy gap of this system. In this case, the interference visibility is equal to one.

¹ Identical to applying the Hadamard gate $H = \frac{1}{\sqrt{2}} \begin{bmatrix} 1 & 1 \\ 1 & -1 \end{bmatrix}$ to a qubit state.

III. PARTICLE WITH INTERNAL STATES IN THE EXTERNAL GRAVITATIONAL FIELD

We consider a particle with INT degrees of freedom in the external gravitational field. When the particle is moving slowly in a weak gravitational field, any internal energy contributes to the total rest mass of the particle respecting the mass-energy equivalence as follows:

$$\hat{m} = m_0 \hat{I} + \hat{H}_{\text{INT}}/c^2 \quad (9)$$

Here, m_0 is the rest mass for the CM system, H_{INT} is the Hamiltonian for the INT system, and they satisfy $H_{\text{INT}} \ll m_0 c^2$. Let us assume the particle to have two internal energy levels, namely $E_0 = 0$ and $E_1 = E$. Then by substituting

$$\hat{H}_{\text{INT}} = \sum_{j=0,1} E_j |E_j\rangle \langle E_j|, \quad (10)$$

the total rest mass of the particle is given as

$$\hat{m} = m_0 \hat{I} + \frac{1}{c^2} \sum_{j=0,1} E_j |E_j\rangle \langle E_j|, \quad \hat{I} = \sum_{j=0,1} |E_j\rangle \langle E_j|. \quad (11)$$

The total state of the particle system is described by the CM system and the INT system. The CM system is characterized by its position \mathbf{x} and conjugate momentum \mathbf{p} . The INT system is characterized by its energy eigenstate $|E_j\rangle$. Considering a weak external gravitational field, the metric is given by

$$ds^2 = -(1 + 2\Phi(\mathbf{x})/c^2)dt^2 + (1 - 2\Phi(\mathbf{x})/c^2)d\mathbf{x}^2, \quad (12)$$

where $\Phi(\mathbf{x})$ is the gravitational potential with $|\Phi|/c^2 \ll 1$. In general, the Hamiltonian of a free-falling particle with its mass m on the background spacetime is

$$H = \sqrt{-g_{00}(m^2 c^4 + c^2 g_{ij} p^i p^j)}.$$

This time, since we consider the particle whose mass depends on the internal energy level as in (11), and assume that the system is on a less relativistic scale, we obtain

$$H \approx H_{\text{CM}} + (1 + \Gamma(\mathbf{x}, \mathbf{p})/c^2) H_{\text{INT}}, \quad \Gamma(\mathbf{x}, \mathbf{p}) := -\frac{\mathbf{p}^2}{2m_0^2} + \Phi(\mathbf{x}) \quad (13)$$

as a lowest order approximation in Taylor expansion of $1/c^2 \ll 1$ and $H_{\text{INT}}/(m_0 c^2) \ll 1$. Here, H_{CM} is the CM Hamiltonian whose explicit form is

$$H_{\text{CM}} = m_0 + \frac{\mathbf{p}^2}{2m_0} + m_0 \Phi(\mathbf{x}), \quad (14)$$

H_{INT} is the INT Hamiltonian given in (10), and Γ is the red-shift factor. We take a unit of $c = 1$ in the following.

Using Eq. (13), if the particle is trapped in a harmonic potential with the stiffness constant k , the total Hamiltonian can be written as follows [8]:

$$\begin{aligned} \hat{H} &= \hat{m} + \frac{\hat{p}^2}{2\hat{m}} + \hat{m} \hat{\Phi}(\hat{x}) + \frac{k}{2} \hat{x}^2 \\ &= \sum_{j=0,1} \left[m_j + \frac{\hat{p}^2}{2m_j} + m_j \hat{\Phi}(\hat{x}) + \frac{m_j \omega_j^2}{2} \hat{x}^2 \right] \otimes |E_j\rangle \langle E_j| = \sum_{j=0,1} \hat{H}_j \otimes |E_j\rangle \langle E_j|, \end{aligned} \quad (15)$$

where $\omega_j = (k/m_j)^{1/2}$. Note that the internal energy level E_0, E_1 are eigenvalues of H_{INT} , and they have nothing to do with an infinite number of energy eigenvalues of H_{CM} since the INT and CM systems are orthogonal. To see that the particle system consists of two independent systems, CM and INT, explicitly, we can rewrite Eq. (15) as

$$\hat{H} = \sum_{j=0,1} \left\{ \sum_{n=0}^{\infty} (m_j + \hbar \omega_j (n + 1/2)) |n_j\rangle \langle n_j| \right\} \otimes |E_j\rangle \langle E_j| \quad (16)$$

where n labels the energy eigenvalues of the CM system, and $|n_j\rangle$ is the n th eigenstate of the CM system for \hat{H}_j .

Figure 2 displays the setup for the external gravitational potential $\hat{\Phi}$, which form depends on whether gravity creates the quantum entanglement or not. The gravitational source mass is placed at $d + \hat{X}$. In Sec. IV we will consider that the gravitational source is spacially superposed at $X = \pm\beta$.

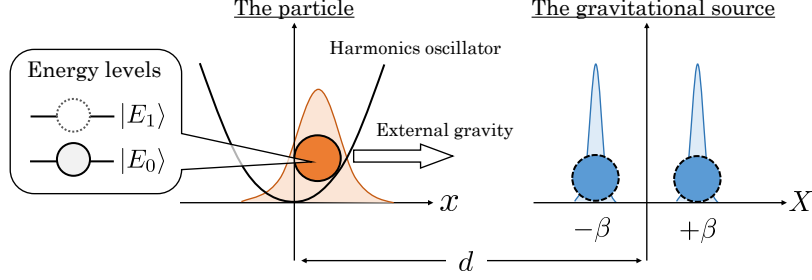


FIG. 2. Setup for the proposed method. The gravitational source is placed at $X = \pm\beta$ as a quantum mechanically superposed state (cat state), and a trapped particle with internal energy levels interacts with it.

We first focus on the case when gravity produces the quantum entanglement between the particle and the gravitational source systems. We will consider a specific form of the Newtonian potential which contains both the operators of the particle and the gravitational source systems, which we call quantized Newtonian gravity (QG) throughout the text. Note that quantized Newtonian gravity does not immediately imply the Newtonian limit of quantum gravity theory, but we adopt it as a particular gravitational interaction that produces entanglement. The QG potential is given as

$$\hat{\Phi} = \frac{-GM}{d + \hat{X} - \hat{x}} \approx -\frac{GM}{d} \left\{ 1 + \frac{\hat{x} - \hat{X}}{d} + \left(\frac{\hat{x} - \hat{X}}{d} \right)^2 \right\} \quad (17)$$

$$= -A(\hat{X}) - B(\hat{X})\hat{x} - C\hat{x}^2, \quad (18)$$

where

$$A(\hat{X}) := \frac{GM}{d} \left(1 - \frac{\hat{X}}{d} + \frac{\hat{X}^2}{d^2} \right), \quad B(\hat{X}) := \frac{GM}{d^2} \left(1 - \frac{2\hat{X}}{d} \right), \quad C := \frac{GM}{d^3}. \quad (19)$$

In the second equality of Eq. (17), we performed Taylor expansion for $d \gg |\langle \hat{X}^n \rangle|, |\langle \hat{x}^n \rangle|$ ($n = 0, 1, 2, \dots$). Therefore, the Hamiltonian is

$$\hat{H}_{\text{QG}} = \sum_{j=0,1} \left[\mathcal{E}_j(\hat{X}) + \frac{\hat{p}^2}{2m_j} + \frac{m_j \omega_j^2}{2} (\hat{x} - \Delta_j(\hat{X}))^2 \right] |E_j\rangle \langle E_j|, \quad (20)$$

where

$$\mathcal{E}_j(\hat{X}) := m_j \left(1 - A(\hat{X}) - \frac{B^2(\hat{X})}{2\omega_j^2} \right), \quad \Delta_j(\hat{X}) := B(\hat{X})/\omega_j^2. \quad (21)$$

Herein, we redefined a shifted angular frequency as $\omega_j^2 - C \rightarrow \omega_j^2$. $\mathcal{E}_j(\hat{X})$ represents the offset of the total energy of the CM system with the j th INT state, and $\Delta_j(\hat{X})$ represents the shift in the harmonic potential due to the weak external gravitational field.

The information of source position \hat{X} is included in $\mathcal{E}_j(\hat{X})$ and $\Delta_j(\hat{X})$, which indicates the entanglement between the CM system \hat{x} and the gravitational source (S) system \hat{X} . Moreover, since the INT system also couples with the CM system and S system as well, the total system is in a tripartite entangled state. In particular, the entanglement between the INT system and S system is uniquely induced by the gravitational coupling $\hat{m} \hat{\Phi}(\hat{x}, \hat{X})$; No other quantum interaction can create this entanglement since they do not couple to the mass \hat{m} due to the weak equivalence principle. Further discussion will be given in Sec. VI. Figure 3 displays a schematic representation of the potential of Hamiltonian

\hat{H}_j . Shifts of the vertex height and the symmetry axis of the potential depend on INT states and this behavior is caused by the coupling between the CM system and INT system via the weak external gravitational field. Section IV will discuss that these shifts of the potential result in collapse and revival of interferometric visibility, which can be interpreted as the universal decoherence of the INT state via external gravitational field [4, 6].

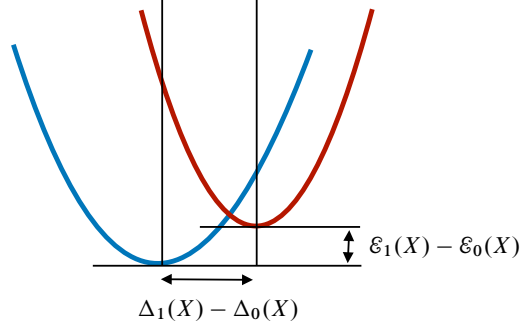


FIG. 3. Schematic representation of the potential for CM degrees of freedom. Blue curve: the potential of \hat{H}_0 . Red curve: the potential of \hat{H}_1 . Shifts in the symmetry axis and the vertex height of the potential are caused by the differences $\Delta_1(X) - \Delta_0(X)$ and $\mathcal{E}_1(X) - \mathcal{E}_0(X)$. The difference in the vertex height depends on the location of the gravitational source X .

In the semiclassical treatment of gravity, hereafter referred to as classical gravity (CG), $\hat{\Phi}$ is replaced by the expectation value concerning the state of the gravitational source $\langle \hat{\Phi} \rangle_S = \langle \varphi_S | \hat{\Phi} | \varphi_S \rangle$ which does not create quantum entanglement between the particle and the gravitational source systems, unlike the QG case. Therefore, for $d \gg |\langle \hat{X}^n \rangle_S|, |\langle \hat{x}^n \rangle|$ ($n = 0, 1, 2, \dots$), the gravitational potential is approximately given by

$$\hat{\Phi} = \left\langle \frac{-GM}{d + \hat{X} - \hat{x}} \right\rangle_S \approx -\frac{GM}{d} \left\{ 1 + \frac{\hat{x} - \langle \hat{X} \rangle_S}{d} + \frac{\hat{x}^2 - 2\langle \hat{X} \rangle_S \hat{x} + \langle \hat{X}^2 \rangle_S}{d^2} \right\} \quad (22)$$

$$= -A - B\hat{x} - C\hat{x}^2, \quad (23)$$

where

$$A := \frac{GM}{d} \left(1 - \frac{\langle \hat{X} \rangle_S}{d} + \frac{\langle \hat{X}^2 \rangle_S}{d^2} \right), \quad B := \frac{GM}{d^2} \left(1 - \frac{2\langle \hat{X} \rangle_S}{d} \right), \quad C := \frac{GM}{d^3}. \quad (24)$$

Therefore, the corresponding Hamiltonian becomes

$$\hat{H}_{CG} = \sum_{j=0,1} \left[\mathcal{E}_j + \frac{\hat{p}^2}{2m_j} + \frac{m_j \omega_j^2}{2} (\hat{x} - \Delta_j)^2 \right] |E_j\rangle \langle E_j|, \quad (25)$$

where

$$\mathcal{E}_j = m_j \left(1 - A - \frac{B^2}{2\omega_j^2} \right), \quad \Delta_j = B/\omega_j^2. \quad (26)$$

In the CG case, CM and INT can entangle through relativistic and classical gravitational couplings, while INT and S cannot entangle.

Next, we introduce the annihilation operator for the CM system for later use:

$$\hat{a}_{j,\hat{X}} = \sqrt{\frac{m_j \omega_j}{2}} \left(\hat{x} + i \frac{\hat{p}}{m_j \omega_j} - \Delta_j(\hat{X}) \right). \quad (27)$$

Therefore, the Hamiltonian for the QG case becomes

$$\hat{H}_{QG}(\hat{X}) = \sum_{j=0,1} \left[\mathcal{E}_j(\hat{X}) + \omega_j \left(\hat{a}_{j,\hat{X}}^\dagger \hat{a}_{j,\hat{X}} + \frac{1}{2} \right) \right] |E_j\rangle \langle E_j|. \quad (28)$$

The Hamiltonian of the CG case is obtained by replacing the functions of \hat{X} with the expectation value for the S state, $f(\hat{X}) \rightarrow \langle f(\hat{X}) \rangle_S$, in Eq. (28).

IV. EVOLUTION OF THE PARTICLE STATE AND VISIBILITY

In this section, we evaluate the interference visibility. We assume that the gravitational source state is in superposition of two Gaussian states (See Fig. 2),

$$|\varphi_S\rangle = \frac{1}{\sqrt{N}} (|\varphi_{-\beta}\rangle + |\varphi_{+\beta}\rangle), \quad \varphi_{\pm\beta}(X) = \langle X|\varphi_{\pm\beta}\rangle = \left(\frac{1}{\pi\sigma^2}\right)^{1/4} e^{-(X\mp\beta)^2/(2\sigma^2)}, \quad N = 2(1 + e^{-\beta^2/\sigma^2}), \quad (29)$$

where β is the separation of the cat state and σ is the width of each Gaussian state. The evolution operator associated with the j th INT state can be expressed as

$$e^{-i\varepsilon_j(\hat{X})t} e^{-i\omega_j(\hat{a}_{j,\hat{X}}^\dagger\hat{a}_{j,\hat{X}}+1/2)t} = e^{-i\varepsilon_j(\hat{X})t} \hat{U}_{j,\hat{X}}(t), \quad (30)$$

where $\hat{U}_{j,\hat{X}}(t) = e^{-i\hat{h}_j(\hat{X})t}$ is the evolution operator with the harmonic oscillator Hamiltonian $\hat{h}_j(\hat{X}) := \omega_j(\hat{a}_{j,\hat{X}}^\dagger\hat{a}_{j,\hat{X}} + 1/2)$. As the initial state of the CM system, we prepare the ground state of $\hat{h}_0(X=0)$ as

$$\psi_{\text{ini}}(x) = \left(\frac{a_0}{\pi}\right)^{1/4} \exp\left[-\frac{a_0}{2}(x - \Delta_0(0))^2\right], \quad a_0 = m_0\omega_0. \quad (31)$$

Therefore, the time evolution of the total state associated with the j th INT state becomes

$$|\Psi_j(t)\rangle = e^{-i\varepsilon_j(\hat{X})t} \hat{U}_{j,\hat{X}}(t) |\psi_{\text{ini}}\rangle \otimes |\varphi_S\rangle = \int dX \varphi_S(X) e^{-i\varepsilon_j(X)t} |\psi_{j,X}(t)\rangle \otimes |X\rangle, \quad (32)$$

Here, we defined $|\psi_{j,X}(t)\rangle := \hat{U}_{j,X}(t) |\psi_{\text{ini}}\rangle$. Introducing the propagator of the harmonics oscillator, we obtain

$$\begin{aligned} K_{j,X}(x,t;y,0) &:= \langle x|\hat{U}_{j,X}(t)|y\rangle \\ &= \sqrt{\frac{a_j}{2\pi i \sin(\omega_j t)}} \exp\left[\frac{ia_j}{2\sin(\omega_j t)} \left\{((x - \Delta_j(X))^2 + (y - \Delta_j(X))^2) \cos(\omega_j t) - 2(x - \Delta_j(X))(y - \Delta_j(X))\right\}\right], \end{aligned} \quad (33)$$

and the wave function of the CM state can be explicitly calculated as [27]

$$\begin{aligned} \psi_{j,X}(x,t) &= \langle x|\hat{U}_{j,X}(t)|\psi_{\text{ini}}\rangle = \int dy \langle x|\hat{U}_{j,X}(t)|y\rangle \langle y|\psi_{\text{ini}}\rangle = \int dy K_{j,X}(x,t;y,0) \psi_{\text{ini}}(y) \\ &= \left(\frac{a_0}{\pi}\right)^{1/4} \sqrt{\frac{a_j}{a_j \cos(\omega_j t) + ia_0 \sin(\omega_j t)}} \exp\left[-\frac{a_j^2}{2a_0} \frac{R_{j,X}(t,x) + iI_{j,X}(t,x)}{1 + (a_j^2/a_0^2 - 1) \cos^2(\omega_j t)}\right], \end{aligned} \quad (34)$$

where $a_j := m_j\omega_j$ and

$$R_{j,X}(t,x) := \left[(x - \Delta_j(X)) - (\Delta_0(X) - \Delta_j(X)) \cos(\omega_j t)\right]^2, \quad (35)$$

$$\begin{aligned} I_{j,X}(t,x) &:= -\sin(\omega_j t) \left[\frac{a_0}{a_j} \left\{((x - \Delta_j(X))^2 + (\Delta_0(X) - \Delta_j(X))^2) \cos(\omega_j t) - 2(x - \Delta_j(X))(\Delta_0(X) - \Delta_j(X))\right\}\right. \\ &\quad \left. - \frac{a_j}{a_0} (x - \Delta_j(X))^2 \cos(\omega_j t)\right]. \end{aligned} \quad (36)$$

To obtain the transition probability Eq. (7), we should evaluate

$$\langle\Psi_0(t)|\Psi_1(t)\rangle = \int dX |\varphi_S(X)|^2 e^{-i(\varepsilon_1(X) - \varepsilon_0(X))t} \langle\psi_{0,X}(t)|\psi_{1,X}(t)\rangle. \quad (37)$$

The source state is assumed to be prepared as Eq. (29) to reveal quantum superposition on gravity, and has no dynamics for simplicity of treatment. Furthermore, the S system is regarded as a two-level state with $X = \pm\beta$. Therefore, Eq. (32) reduces to the following expression,

$$|\Psi_j(t)\rangle \approx \frac{1}{\sqrt{N}} \sum_{s=\pm\beta} e^{-i\varepsilon_j(s)t} |\psi_{j,s}(t)\rangle \otimes |\varphi_s\rangle. \quad (38)$$

Herein, we made the assumption that $\psi_{j,X}(t, x)$ and $e^{-i\mathcal{E}_j(X)t}$ in Eq. (32) do not change rapidly with respect to X within the width σ of the Gaussian function in $\varphi_S(X)$. Each assumption requires the following condition respectively,

$$a_j \left(\frac{GM}{\omega^2 d^3} \right)^2 \ll \frac{1}{\sigma^2}, \quad \frac{Gm_j M}{d^3} t \ll \frac{1}{\sigma^2}. \quad (39)$$

The former inequality is satisfied when the Gaussian dispersion of the CM system and the source system are in the same order, and the displacement of the CM state is relatively small compared to d : $\frac{GM}{\omega^2 d^3} \sim \Delta_j/d \ll 1$. The latter inequality gives the upper bound of the valid time range t for the form of the state expressed in Eq. (38). Then Eq. (37) is approximately given as a summation of four terms,

$$\langle \Psi_0(t) | \Psi_1(t) \rangle \approx \frac{1}{N} \sum_{s_1, s_2 = \pm\beta} \langle \varphi_{s_1} | \varphi_{s_2} \rangle e^{-i(\mathcal{E}_1(s_2) - \mathcal{E}_0(s_1))t} \langle \psi_{0,s_1}(t) | \psi_{1,s_2}(t) \rangle. \quad (40)$$

Figure 4 depicts a schematic picture of the Ramsey interferometry under quantum gravity (QG). Since the CM state depends not only on the INT energy level E_i but also the gravitational source position $X = \pm\beta$, its time evolution is given by a superposition of four different worldline branches (Additional details regarding the states involved in the interference visibility are given in Appendix A).

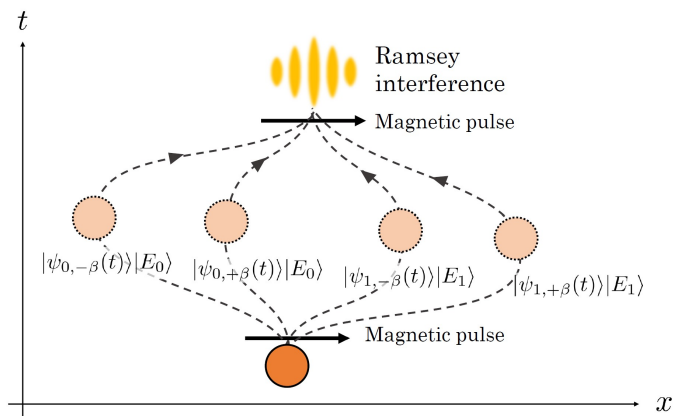


FIG. 4. Schematic picture of Ramsey interferometry in the QG case. Four different worldline branches are involved in interference visibility.

For the CG case, the Ramsey interferometry is derived analogously by replacing the functions of \hat{X} with the expectation value of $f(\hat{X}) \rightarrow \langle f(\hat{X}) \rangle_S$. Then, Eq. (37) can be expressed as

$$\langle \Psi_0(t) | \Psi_1(t) \rangle = e^{-i(\mathcal{E}_1 - \mathcal{E}_0)t} \langle \psi_0(t) | \psi_1(t) \rangle, \quad (41)$$

where \mathcal{E}_j is as per in Eq. (26), and $|\psi_j(t)\rangle := e^{-i\hat{h}_j t} |\psi_{\text{ini}}\rangle$ is the time evolved CM state with the harmonics oscillator Hamiltonian for CG $\hat{h}_j := \langle \hat{h}_j(\hat{X}) \rangle_S$. The Ramsey interferometry under CG is depicted in Fig. 1. We see that the time evolution of the CM system is given by a superposition of two worldline branches concerning the INT energy levels E_0 or E_1 .

Although it is possible to derive an explicit but complicated formula of Eq. (40) using a straightforward calculation of the Gaussian integral, we only present the plotting results in subsequent figures Figs. 5, 6, 7, and 11. Instead, in the following, we derive an approximate analytical form of Eq. (37) by focusing only up to the leading term of the Taylor expansion of the gravitational potential expressed in Eq. (18), which helps our qualitative understanding of gravity-induced decoherence. If we neglect the subleading terms of the Taylor expansion parameters x/d and X/d in (18), Eq. (19) can be expressed as

$$A(\hat{X}) \rightarrow \frac{GM}{d} \left(1 - \frac{\hat{X}}{d} \right), \quad B(\hat{X}) \rightarrow \frac{GM}{d^2}, \quad C \rightarrow 1. \quad (42)$$

Herein, the \hat{X} dependence only appears in $\mathcal{E}_j(\hat{X})$, and the coupling of the CM system operator \hat{x} and the S system operator \hat{X} disappears as $\Delta_j(\hat{X}) \rightarrow \Delta_j$. Although the BMV proposal [9, 10] focuses on the entanglement between the CM system and S system, this study aims to investigate the entanglement between the INT system and S system, which is uniquely induced by gravitational coupling due to the weak equivalence principle. (Further details will be revisited in Sec. VI.) Therefore, this approximation is enough to capture the crucial effect of the quantumness of gravity in our setup of the Ramsey interferometry.

Since \hat{h}_j does not depend on \hat{X} for now, the X integration in Eq. (37) can be simplified to

$$\langle \Psi_0(t) | \Psi_1(t) \rangle = \langle \psi_0(t) | \psi_1(t) \rangle \times \int dX |\varphi_S(X)|^2 e^{-i(\mathcal{E}_1(X) - \mathcal{E}_0(X))t}. \quad (43)$$

Evaluating the inner product of CM states $\langle \psi_0(t) | \psi_1(t) \rangle$ with (42), we obtain

$$\langle \psi_0(t) | \psi_1(t) \rangle = \int dx \psi_0^*(t, x) \psi_1(t, x) =: |\mathcal{V}_C(t)| e^{i\Theta_C(t)}, \quad (44)$$

where

$$|\mathcal{V}_C(t)| = \left(\frac{4a_0 a_1}{4a_0 a_1 \cos^2(\omega_1 t) + (a_0 + a_1)^2 \sin^2(\omega_1 t)} \right)^{1/4} \exp \left[-\frac{2a_0 a_1^2 (\Delta_0 - \Delta_1)^2 \sin^2(\omega_1 t/2)}{a_0^2 + a_1^2 + (a_0^2 - a_1^2) \cos(\omega_1 t)} \right], \quad (45)$$

$$\Theta_C(t) = -\frac{a_0 a_1^2 (\Delta_0 - \Delta_1)^2 \sin(\omega_1 t)}{a_0^2 + a_1^2 + (a_0^2 - a_1^2) \cos(\omega_1 t)} - \frac{1}{2} \arg \left[e^{-i\omega_0 t} (2a_0/a_1 \cos(\omega_1 t) + i(1 + (a_0/a_1)^2) \sin(\omega_1 t)) \right]. \quad (46)$$

It should be noted that $\mathcal{V}_C(t)$ is a $2\pi/\omega_1$ periodic function in time t that reflects the oscillation of the CM state in the harmonic oscillator potential. The X integration in Eq. (43) reads to

$$\int dX |\varphi_S(X)|^2 e^{-i(\mathcal{E}_1(X) - \mathcal{E}_0(X))t} = |\mathcal{V}_Q(t)| e^{i\Theta_\mathcal{E}(t)}, \quad (47)$$

where

$$|\mathcal{V}_Q(t)| = \frac{2}{N} \exp \left[-\left(\frac{GME \sigma}{2d} \frac{\sigma}{d} t \right)^2 \right] \left| \cos \left(\frac{GME \beta}{d} \frac{\beta}{d} t \right) + e^{-\beta^2/\sigma^2} \right|, \quad (48)$$

$$\Theta_\mathcal{E}(t) = -(\mathcal{E}_1(0) - \mathcal{E}_0(0))t. \quad (49)$$

Finally, when we treat up to the leading term of x/d , X/d , the analytic expression of Eq. (37) is given by

$$\langle \Psi_0(t) | \Psi_1(t) \rangle = |\mathcal{V}_C(t) \mathcal{V}_Q(t)| e^{i(\Theta_C(t) + \Theta_\mathcal{E}(t))} \quad (\text{QG case}), \quad (50)$$

where the time-dependent functions $|\mathcal{V}_C|, \Theta_C, |\mathcal{V}_Q|, \Theta_\mathcal{E}$ are given in Eqs. (45), (46), (48), and (49), respectively. For the CG case, the treatment can be applied by replacing $\hat{X} \rightarrow \langle X \rangle = 0$, which reduces the X integration in Eq. (47) to 1, and we get the final expression for the inner product as

$$\langle \Psi_0(t) | \Psi_1(t) \rangle = |\mathcal{V}_C(t)| e^{i(\Theta_C(t) + \Theta_\mathcal{E}(t))} \quad (\text{CG case}). \quad (51)$$

Let us discuss some properties of interference for different treatments of gravity based on Eqs. (50) and (51) in the following.

First, when there is no external gravitational source ($G = 0$ and $\Delta_0 = \Delta_1 = 0$), the probability oscillates with a period determined by the energy gap of the INT system $\mathcal{E}_1 - \mathcal{E}_0 = E$. The envelope of the oscillation is determined by visibility $|\mathcal{V}_C(t)|$, whose time period π/ω_1 reflects the evolution of the squeezed state, as seen Eq. (46) (and also in Appendix A). The decoherence arises from the entanglement between the CM system and INT systems induced by the kinetic term. In other words, a particle with a different energy level evolves along a different branch of world line with a different proper times due to the special relativistic redshift, as seen in Fig. 1, which results in universal decoherence [4].

For the CG case, the visibility factor $|\mathcal{V}_C(t)|$ contains two typical periods: (i) π/ω_1 , which corresponds to the period of squeezed state, and (ii) $2\pi/\omega_1$, which corresponds to the period of coherent state originated from the interaction of the CM state with the external CG [8] (see also Appendix A). Each periodic decoherence behavior in CG occurs due to the entanglement between the CM and the INT systems induced by the kinetic term, and the semiclassical gravitational interaction; the later refers to universal decoherence caused by a gravitational redshift [4]. In the left

panel of Fig. 5, we show the time dependence of the probability $P(t)$ under CG with a green solid line, which is obtained by evaluating Eq. (41). It exhibits oscillation with a period $\approx 2\pi/(\mathcal{E}_1 - \mathcal{E}_0)$, which roughly corresponds to the energy gap of the INT system with relativistic and gravitational corrections. The dashed lines denote its envelope $(1 + |\mathcal{V}_C(t)|)/2$, and parameters are chosen as $(m_0^3/k)^{1/2} = 10$, $(m_0/m_1)^{1/2} = 0.5$, $Gm_0M/(kd^3) = 0.015$, $m_0^{1/4}d = 10$, $\beta/d = 0.01$, $\sigma/d = 0.001$. The visibility again exhibits revival behavior with the $2\pi/\omega_1$ period, thereby reflecting semi-classical gravity induced entanglement.

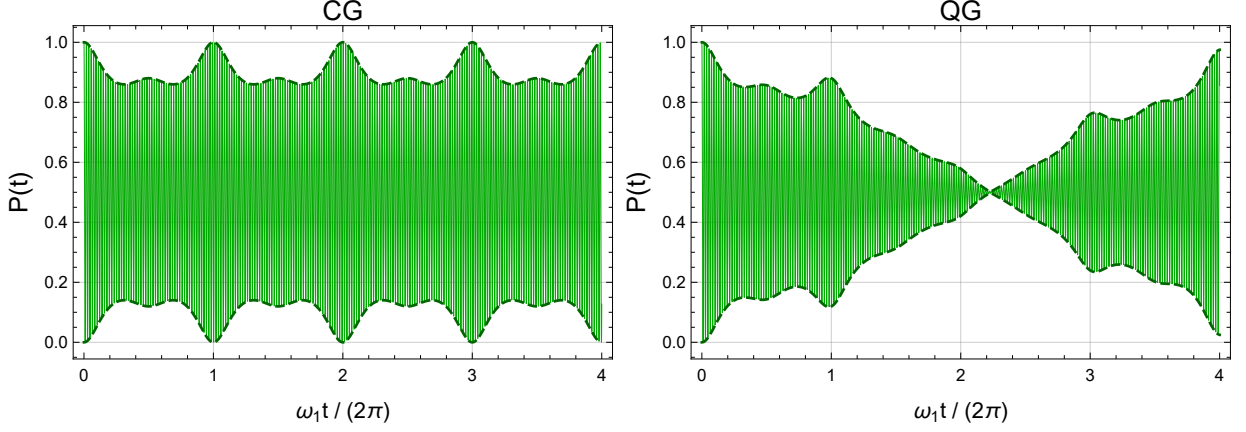


FIG. 5. Probability $P(t)$ of the CG case (left panel) and QG case (right panel). Solid line: time dependence of the probability $P(t)$. Dashed line: the envelope of $P(t)$, which is $\frac{1}{2}(1 + |\mathcal{V}(t)|)$.

Next, we conduct an in-depth evaluation of the visibility of the QG case in detail as the main result of this study and clarify the effect of the quantum superposition of the gravitational source on the visibility of the Ramsey interferometry. As an effect of the quantumness of gravity, the visibility additionally contains $|\mathcal{V}_Q(t)|$. Furthermore, a modulation with a longer period appears in the visibility due to the following reasons: (i) the exponential factor in $|\mathcal{V}_Q(t)|$ of Eq. (48) causes the temporal decay of coherence. It contains the gravitational coupling between the source mass and the INT energy gap and vanishes for $\sigma \rightarrow 0$. This indicates the entanglement induced by the quantum gravitational interaction between the INT system and the Gaussian dispersion of the S system. Since its decoherence time scale is given by $t \sim \left(\frac{GME}{2d} \frac{\sigma}{d}\right)^{-1}$, the system decoheres more rapidly for larger σ . (ii) The product of two kinds of periodic functions, namely the cosine function in $\mathcal{V}_Q(t)$ and the function $\mathcal{V}_C(t)$ with a period $2\pi/\omega_1$ causes a beat in the visibility. The cosine function in $\mathcal{V}_Q(t)$ comes from the gravitational coupling between the source mass and the INT energy gap, and it vanishes for $\beta \rightarrow 0$. This indicates the entanglement induced by the quantum gravitational interaction between the INT system and the distant cat state. Since its decoherence time scale is given by $t \sim \left(\frac{GME}{d} \frac{\beta}{d}\right)^{-1}$, the system decoheres more rapidly for larger β .

Decoherence effect (i) is caused by the Gaussian spread of the source mass state, and causes nonrevival behavior of the visibility. It is induced by the entanglement between the INT state $|E_j\rangle$ and the Gaussian state $\int dX e^{-X^2/2\sigma^2} |X\rangle$ with infinite rank. Decoherence effect (ii) is induced by the entanglement between the INT state and the distant cat state $|\pm\beta\rangle$ with rank 2. Therefore, the combination of the INT state and the distant cat state subsystem mentioned in (ii) is much easier to get entangled compared to the combination of the INT state $|E_j\rangle$ and the Gaussian state $\int dX e^{-X^2/2\sigma^2} |X\rangle$ with infinite rank mentioned in (i). To summarize, the quantumness of gravity is reflected in the visibility as a nonrevival behavior of visibility (coherence), which is induced by the entanglement between the INT system and the S system as mentioned in Sec. III.

In the right panel of Fig. 5, we showed the time dependence of the probability $P(t)$ for the QG case with a solid line, and its envelope $(1 + |\mathcal{V}_C(t)\mathcal{V}_Q(t)|)/2$ with a dotted line. The parameters are set to $(m_0^3/k)^{1/2} = 10$, $(m_0/m_1)^{1/2} = 0.5$, $Gm_0M/(kd^3) = 0.015$, $m_0^{1/4}d = 10$, $\beta/d = 0.01$, $\sigma/d = 0.001$. The figure displays the beat in the envelope of its oscillation, and unlike the CG case, the visibility does not exhibit revival behavior. It should be noted that the exponential decay in $\mathcal{V}_{QG}(t)$ obtained in Eq. (48) is not obvious here, since the exponential factor in Eq. (37) is not dominant in the integral unless a time t violates the condition expressed in Eq. (39).

Finally, the behavior of visibility is explored by comparing the CG and QG cases displayed in Fig. 6. The blue and red lines denote the CG case and QG case respectively. The parameters are identical to those mentioned in Fig. 5. As per the figure, the visibility of QG returns to nearly one after a period of $(GME\beta/d^2)^{-1}$, while its value decays by $\exp(-(GME\sigma t/2d^2)^2)$, as estimated in Eq. (48). To summarize, the quantumness of gravity appears as a nonrevival

behavior of interference visibility. Stronger decoherence in QG compared to that in CG indicates the entanglement sharing between the particle and S systems.

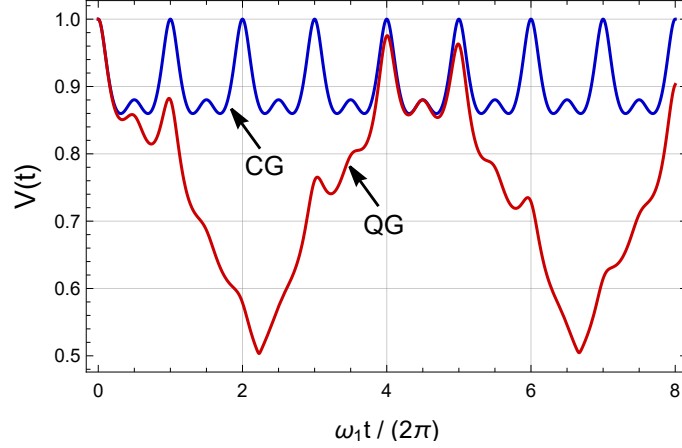


FIG. 6. Visibility for the CG case (blue line) and the QG case (red line). Owing to the decoherence effect induced by the spread of the source state, the visibility of QG does not come back to unity and does not show revival behavior.

V. NEGATIVITY OF REDUCED BIPARTITE STATES

In this section, we will evaluate the entanglement between the CM, INT, and the gravitational source systems, which provide a better understanding of the decoherence in the Ramsey interference mentioned in Sec. IV. The state of the total system is given by

$$|\Psi(t)\rangle = \frac{1}{\sqrt{2}} \sum_{j=0,1} e^{-i\mathcal{E}_j(\hat{X})t} |E_j\rangle \otimes |\psi_{j,\hat{X}}(t)\rangle \otimes |\varphi_S\rangle. \quad (52)$$

To see the entanglement structure during the collapse and revival of coherence in Fig. 6, we assumed the same approximation adopted in Sec. IV for Eq. (39). As preparation, the CM states and the source Gaussian state are rewritten as

$$\begin{bmatrix} |C_0\rangle \\ |C_1\rangle \\ |C_2\rangle \\ |C_3\rangle \end{bmatrix} = \begin{bmatrix} |C_{J[0,0]}\rangle \\ |C_{J[0,1]}\rangle \\ |C_{J[1,0]}\rangle \\ |C_{J[1,1]}\rangle \end{bmatrix} := \begin{bmatrix} |\psi_{0,-\beta}\rangle \\ |\psi_{0,+\beta}\rangle \\ |\psi_{1,-\beta}\rangle \\ |\psi_{1,+\beta}\rangle \end{bmatrix}, \quad \begin{bmatrix} |S_0\rangle \\ |S_1\rangle \end{bmatrix} := \begin{bmatrix} |\varphi_{-\beta}\rangle \\ |\varphi_{+\beta}\rangle \end{bmatrix}, \quad (53)$$

where we define a the function $J[j, k] := 2j + k = \{0, 1, 2, 3\}$, and the offset of the total energy $\mathcal{E}_{J[j,k]} := \mathcal{E}_j((2k-1)\beta)$. The state of the total system is expressed as

$$|\Psi(t)\rangle = \frac{1}{\sqrt{2N}} \sum_{j=0,1} \sum_{k=0,1} e^{-i\mathcal{E}_{J[j,k]}t} |E_j\rangle \otimes |C_{J[j,k]}\rangle \otimes |S_k\rangle. \quad (54)$$

Therefore, the density matrix of the total system is obtained as

$$\rho = |\Psi\rangle \langle\Psi| = \frac{1}{2N} \sum_{j_1, j_2} \sum_{k_1, k_2} e^{-i(\mathcal{E}_{J[j_1, k_1]} - \mathcal{E}_{J[j_2, k_2]})t} |E_{j_1}\rangle \langle E_{j_2}| \otimes |C_{J[j_1, k_1]}\rangle \langle C_{J[j_2, k_2]}| \otimes |S_{k_1}\rangle \langle S_{k_2}|. \quad (55)$$

We considered three different reduced bipartite states as follows:

$$\rho_{\text{INT:CM}} := \text{Tr}_S \rho = \frac{1}{2N} \sum_{j_1, j_2, k_1, k_2} e^{-i(\mathcal{E}_{J[j_1, k_1]} - \mathcal{E}_{J[j_2, k_2]})t} \langle S_{k_2} | S_{k_1} \rangle |E_{j_1}\rangle \langle E_{j_2}| \otimes |C_{J[j_1, k_1]}\rangle \langle C_{J[j_2, k_2]}|, \quad (56)$$

$$\rho_{\text{INT:S}} := \text{Tr}_{\text{CM}} \rho = \frac{1}{2N} \sum_{j_1, j_2, k_1, k_2} e^{-i(\mathcal{E}_{J[j_1, k_1]} - \mathcal{E}_{J[j_2, k_2]})t} \langle C_{J[j_2, k_2]} | C_{J[j_1, k_1]} \rangle |E_{j_1}\rangle \langle E_{j_2}| \otimes |S_{k_1}\rangle \langle S_{k_2}|, \quad (57)$$

$$\rho_{\text{CM:S}} := \text{Tr}_{\text{INT}} \rho = \frac{1}{2N} \sum_{j, k_1, k_2} e^{-i(\mathcal{E}_{J[j, k_1]} - \mathcal{E}_{J[j, k_2]})t} |S_{k_1}\rangle \langle S_{k_2}| \otimes |C_{J[j, k_1]}\rangle \langle C_{J[j, k_2]}|. \quad (58)$$

To evaluate the negativity for the reduced states, we introduced an orthonormal basis for the S state and the CM state. For the source state, using the orthonormal basis $\{|s_k\rangle\}$, $k = \{0, 1\}$, $\langle s_{k_1}|s_{k_2}\rangle = \delta_{k_1 k_2}$, we obtain

$$\begin{bmatrix} |S_0\rangle \\ |S_1\rangle \end{bmatrix} = \frac{1}{\sqrt{2}} \begin{bmatrix} \sqrt{1+v_S} & \sqrt{1-v_S} \\ \sqrt{1+v_S} & -\sqrt{1-v_S} \end{bmatrix} \begin{bmatrix} |s_0\rangle \\ |s_1\rangle \end{bmatrix}, \quad v_S = \langle S_0|S_1\rangle = e^{-\beta^2/\sigma^2}. \quad (59)$$

This relation is written using a 2×2 matrix S as $|S_k\rangle = \sum_{\ell=0,1} S_{k\ell} |s_\ell\rangle$. For the CM state $|C_{J[j,k]}\rangle$, the orthonormal basis $\{|c_J\rangle\}$, $J = \{0, 1, 2, 3\}$, $\langle c_{J_1}|c_{J_2}\rangle = \delta_{J_1 J_2}$ is obtained using the Gram-Schmidt orthonormalization as follows:

$$\begin{bmatrix} |C_0\rangle \\ |C_1\rangle \\ |C_2\rangle \\ |C_3\rangle \end{bmatrix} = \begin{bmatrix} \sqrt{N_0} & 0 & 0 & 0 \\ \langle c_0|\psi_1\rangle & \sqrt{N_1} & 0 & 0 \\ \langle c_0|\psi_2\rangle & \langle c_1|\psi_2\rangle & \sqrt{N_2} & 0 \\ \langle c_0|\psi_3\rangle & \langle c_1|\psi_3\rangle & \langle c_2|\psi_3\rangle & \sqrt{N_3} \end{bmatrix} \begin{bmatrix} |c_0\rangle \\ |c_1\rangle \\ |c_2\rangle \\ |c_3\rangle \end{bmatrix}, \quad N_J = 1 - \sum_{0 \leq K \leq J-1} |\langle c_K|\psi_J\rangle|^2. \quad (60)$$

Equivalently, the CM state can be expressed as $|\psi_J\rangle = \sum_{K=0,1,2,3} \mathcal{U}_{JK} |c_K\rangle$ using a 4×4 matrix \mathcal{U}_{JK} . Therefore, the reduced states are

$$\rho_{\text{INT:CM}} = \frac{1}{2N} \sum_{j_1 j_2, k_1 k_2} e^{-i(\mathcal{E}_{J[j_1, k_1]} - \mathcal{E}_{J[j_2, k_2]})t} \left(\sum_{\ell} S_{k_1 \ell}^* S_{k_2 \ell} \right) |E_{j_1}\rangle \langle E_{j_2}| \otimes \sum_{K_1 K_2} \mathcal{U}_{J[j_1, k_1] K_1} \mathcal{U}_{J[j_2, k_2] K_2}^* |c_{K_1}\rangle \langle c_{K_2}|, \quad (61)$$

$$\rho_{\text{INT:S}} = \frac{1}{2N} \sum_{j_1 j_2, k_1 k_2} e^{-i(\mathcal{E}_{J[j_1, k_1]} - \mathcal{E}_{J[j_2, k_2]})t} \left(\sum_K \mathcal{U}_{J[j_1, k_1] K} \mathcal{U}_{J[j_2, k_2] K} \right) |E_{j_1}\rangle \langle E_{j_2}| \otimes \sum_{\ell_1 \ell_2} S_{k_1 \ell_1} S_{k_2 \ell_2}^* |s_{\ell_1}\rangle \langle s_{\ell_2}|, \quad (62)$$

$$\rho_{\text{CM:S}} = \frac{1}{2N} \sum_{j, k_1 k_2} e^{-i(\mathcal{E}_{J[j, k_1]} - \mathcal{E}_{J[j, k_2]})t} \sum_{\ell_1 \ell_2} S_{k_1 \ell_1} S_{k_2 \ell_2} |s_{\ell_1}\rangle \langle s_{\ell_2}| \otimes \sum_{K_1 K_2} \mathcal{U}_{J[j, k_1] K_1} \mathcal{U}_{J[j, k_2] K_2}^* |c_{K_1}\rangle \langle c_{K_2}|. \quad (63)$$

The entanglement negativity [28] for a bipartite state is obtained as $\mathcal{N} = \sum_{\lambda_i < 0} |\lambda_i|$ where λ_i is the eigenvalue of the partially transposed density matrix. Logarithmic negativity is defined by

$$N_E := \log_2(2\mathcal{N} + 1), \quad (64)$$

which quantifies the distillable number of Bell pairs.

Figure 7 displays the time dependence of the logarithmic negativity $N_E(t)$ of the reduced bipartite states for the CG and QG cases. The blue, red, and gray line denote entanglement of the CM:INT system, the INT:S system, and CM:S systems respectively. Each entanglement is obtained by evaluating Eqs. (61), (62), and (63). The parameters are identical to those used in Fig. 6, namely $(m_0^3/k)^{1/2} = 10$, $(m_0/m_1)^{1/2} = 0.5$, $Gm_0 M/(kd^3) = 0.015$, $m_0^{1/4} d = 10$, $\beta/d = 0.01$, $\sigma/d = 0.001$. For the CG case, the CM:INT entanglement emerges and disappears for every $2\pi/\omega_1$ period, and the CM:S and S:INT entanglements remain zero. Comparing the CM:INT entanglement with the visibility in Fig. 6 reveals that they both oscillate alternatively with the $2\pi/\omega_1$ period. Therefore, the CM:INT entanglement induced by the relativistic and classical gravitational redshift is reflected in the revival of visibility in the Ramsey interference. For the QG case, whole the CM:INT, INT:S, and CM:S entanglements emerge as time evolves. The CM:S entanglement is relatively smaller than others, because the CM:S entanglement is obtained from the second order of Taylor expansion in Eq. (18), whereas the others originated from the first order. An important effect of the quantumness of gravity appears in the INT:S entanglement which dominates the CM:INT entanglement alternatively during the time evolution. As the source state $|\varphi_{\pm\beta}\rangle$ reduces to a two-level state for $\sigma \rightarrow 0$, the INT:S entanglement can achieve nearly the maximal logarithmic negativity value of one as the reduced state nearly evolves to the Bell state. Moreover, the beat of the visibility in Fig. 6 corresponds exactly to the envelope of the oscillation of the INT:S entanglement. If the CM:S entanglement is neglected, we can conclude that the nonrevival property of the Ramsey interference exactly reflects the creation of the INT:S entanglement revealing the quantumness of gravity.

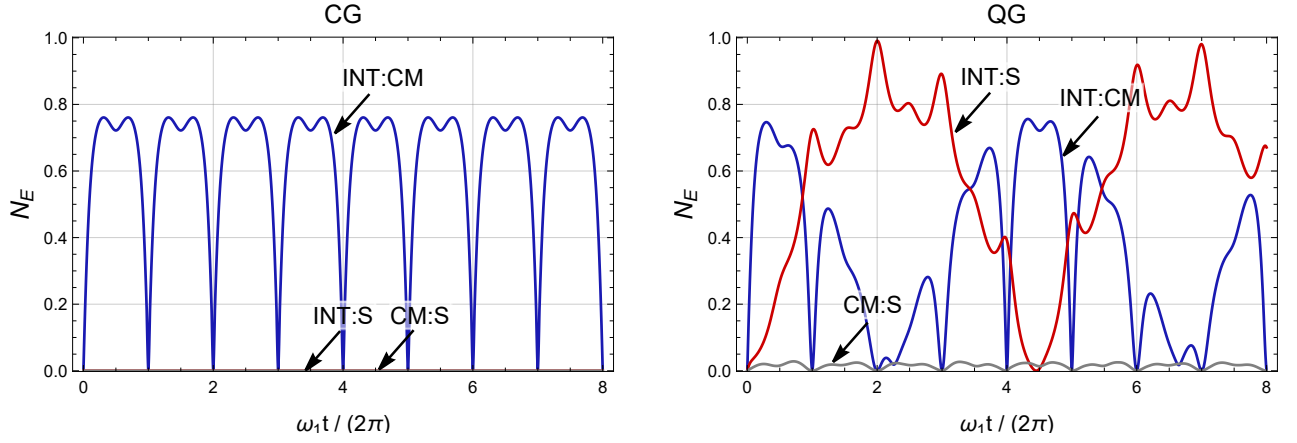


FIG. 7. Logarithmic negativity of reduced bipartite states for CG case (left panel) and QG case (right panel). Bipartite subsystems are denoted as CM:INT (blue line), INT:S (red line) and CM:S (gray line).

As per Fig. 7, CM:S entanglement is negligible under the condition that the Taylor expansion in Eq. (18) is validated. Now, we again consider up to the first order of the Taylor expansion in Eq. (18) to neglect the CM:S entanglement and derive an explicit analytic form of negativity for three different reduced bipartite states to achieve further qualitative understanding. In this approximation, since the dependence of X only appears in \mathcal{E}_j [See also (42)], Eq. (52) becomes

$$|\Psi(t)\rangle = \frac{1}{\sqrt{2}} \sum_{j=0,1} |E_j\rangle \otimes |\tilde{C}_j\rangle \otimes |\tilde{S}_j\rangle, \quad (65)$$

where

$$|\tilde{C}_j\rangle := |\psi_j(t)\rangle, \quad |\tilde{S}_j\rangle := \int dX e^{-i\mathcal{E}_j(X)t} \varphi_S(X)|X\rangle. \quad (66)$$

In particular, in the qubit limit of the CM state and the source state with $\langle \tilde{C}_j | \tilde{C}_k \rangle \rightarrow \delta_{jk}$, $\langle \tilde{S}_j | \tilde{S}_k \rangle \rightarrow \delta_{jk}$, we obtain the Greenberger-Horne-Zeilinger (GHZ) state for the total system as $|\Psi_{\text{GHZ}}\rangle = (|000\rangle + |111\rangle)/\sqrt{2}$. Therefore, the existence of genuine tripartite entanglement for the CM-INT-S state is confirmed. To evaluate the negativity for the reduced states, orthonormal basis $|c_j\rangle$ for the CM state and $|s_j\rangle$ for the S state, which satisfy $\langle c_j | c_k \rangle = \langle s_j | s_k \rangle = \delta_{jk}$ are introduced as follows:

$$\begin{bmatrix} |\tilde{C}_0\rangle \\ |\tilde{C}_1\rangle \end{bmatrix} = \frac{1}{\sqrt{2}} \begin{bmatrix} e^{i\theta_C/2} \sqrt{1+v_C} & e^{i\theta_C/2} \sqrt{1-v_C} \\ e^{-i\theta_C/2} \sqrt{1+v_C} & -e^{-i\theta_C/2} \sqrt{1-v_C} \end{bmatrix} \begin{bmatrix} |c_0\rangle \\ |c_1\rangle \end{bmatrix}, \quad v_C = |\langle \tilde{C}_0 | \tilde{C}_1 \rangle|, \quad \theta_C = \arg[\langle \tilde{C}_0 | \tilde{C}_1 \rangle], \quad (67)$$

$$\begin{bmatrix} |\tilde{S}_0\rangle \\ |\tilde{S}_1\rangle \end{bmatrix} = \frac{1}{\sqrt{2}} \begin{bmatrix} e^{i\theta_S/2} \sqrt{1+v_S} & e^{i\theta_S/2} \sqrt{1-v_S} \\ e^{-i\theta_S/2} \sqrt{1+v_S} & -e^{-i\theta_S/2} \sqrt{1-v_S} \end{bmatrix} \begin{bmatrix} |s_0\rangle \\ |s_1\rangle \end{bmatrix}, \quad v_S = |\langle \tilde{S}_0 | \tilde{S}_1 \rangle|, \quad \theta_S = \arg[\langle \tilde{S}_0 | \tilde{S}_1 \rangle]. \quad (68)$$

Using the orthonormal basis $\{|E_0\rangle, |E_1\rangle, |c_0\rangle, |c_1\rangle, |s_0\rangle, |s_1\rangle\}$, the total state is expressed as

$$\rho = |\Psi\rangle\langle\Psi| = \frac{1}{8} \begin{bmatrix} \mathbf{N}_C \otimes \mathbf{N}_S & e^{i(\theta_C+\theta_S)} \mathbf{N}_C \mathbf{Z} \otimes \mathbf{N}_S \mathbf{Z} \\ e^{-i(\theta_C+\theta_S)} \mathbf{Z} \mathbf{N}_C \otimes \mathbf{Z} \mathbf{N}_S & \mathbf{Z} \mathbf{N}_C \mathbf{Z} \otimes \mathbf{Z} \mathbf{N}_S \mathbf{Z} \end{bmatrix}, \quad (69)$$

where the 2×2 sub-matrices are defined by

$$\mathbf{N}_C = \begin{bmatrix} 1+v_C & \sqrt{1-v_C^2} \\ \sqrt{1-v_C^2} & 1-v_C \end{bmatrix}, \quad \mathbf{N}_S = \begin{bmatrix} 1+v_S & \sqrt{1-v_S^2} \\ \sqrt{1-v_S^2} & 1-v_S \end{bmatrix}, \quad \mathbf{Z} = \begin{bmatrix} 1 & 0 \\ 0 & -1 \end{bmatrix}. \quad (70)$$

Therefore, the three different reduced bipartite states are

$$\rho_{\text{INT:CM}} = \text{Tr}_S \rho = \frac{1}{4} \begin{bmatrix} \mathbf{N}_C & v_S e^{i(\theta_C+\theta_S)} \mathbf{N}_C \mathbf{Z} \\ v_S e^{-i(\theta_C+\theta_S)} \mathbf{Z} \mathbf{N}_C & \mathbf{Z} \mathbf{N}_C \mathbf{Z} \end{bmatrix}, \quad (71)$$

$$\rho_{\text{INT:S}} = \text{Tr}_{\text{CM}} \rho = \frac{1}{4} \begin{bmatrix} \mathbf{N}_S & v_C e^{i(\theta_C+\theta_S)} \mathbf{N}_S \mathbf{Z} \\ v_C e^{-i(\theta_C+\theta_S)} \mathbf{Z} \mathbf{N}_S & \mathbf{Z} \mathbf{N}_S \mathbf{Z} \end{bmatrix}, \quad (72)$$

$$\rho_{\text{CM:S}} = \text{Tr}_{\text{INT}} \rho = \frac{1}{8} (\mathbf{N}_C \otimes \mathbf{N}_S + \mathbf{Z} \mathbf{N}_C \mathbf{Z} \otimes \mathbf{Z} \mathbf{N}_S \mathbf{Z}). \quad (73)$$

As per Eq. (73), $\rho_{\text{CM:S}}$ is separable from its structure. The negativity for reduced bipartite states are

$$\mathcal{N}(\rho_{\text{INT:CM}}) = \frac{1}{4} \left(-1 + v_S + \sqrt{(1 + v_S)^2 - 4v_C^2 v_S} \right), \quad (74)$$

$$\mathcal{N}(\rho_{\text{INT:S}}) = \frac{1}{4} \left(-1 + v_C + \sqrt{(1 + v_C)^2 - 4v_S^2 v_C} \right), \quad (75)$$

$$\mathcal{N}(\rho_{\text{CM:S}}) = 0. \quad (76)$$

Figure 8 displays the dependence of negativities $\mathcal{N}(\rho_{\text{INT:CM}})$, $\mathcal{N}(\rho_{\text{INT:S}})$ on v_S and v_C . For the CG case, since the state is not dependent on X , we have $v_S = 1$. Therefore, $\mathcal{N}(\rho_{\text{INT:S}})$ becomes zero, whereas $\mathcal{N}(\rho_{\text{INT:CM}})$ varies between 0 and 1 depending on values of v_C . For the QG case, since v_S oscillates between 0 and 1, $\mathcal{N}(\rho_{\text{INT:CM}})$ oscillates between 0 and $\sqrt{1 - v_C^2}/2$, whereas $\mathcal{N}(\rho_{\text{INT:S}})$ oscillates between 0 and $v_C/2$; $\mathcal{N}(\rho_{\text{INT:CM}})$ and $\mathcal{N}(\rho_{\text{INT:S}})$ vary alternatively. This implies a monogamous relation of quantum entanglement between the INT:CM systems and INT:S systems, and confirms the existence of genuine tripartite entanglement of the CM-INT-S system.

For the state expressed in Eq. (69), the negativity for the bipartition INT:CM+S of the total state is

$$\mathcal{N}(\rho_{\text{INT:CM+S}}) = \frac{1}{2} \sqrt{1 - v_S^2 v_C^2}, \quad (77)$$

and it obeys monogamy inequality [29] as follows:

$$\mathcal{N}^2(\rho_{\text{INT:CM}}) + \mathcal{N}^2(\rho_{\text{INT:S}}) \leq \mathcal{N}^2(\rho_{\text{INT:CM+S}}). \quad (78)$$

The difference between the sides of this inequality represents the residual entanglement which quantifies genuine tripartite entanglement (right panel of Fig. 8). For the CG case, since $v_S = 1$, there is no residual entanglement. For the QG case, since $v_C \neq 1$ or $v_S \neq 1$, the value of residual entanglement is nonzero. The point $v_C = v_S = 0$ corresponds to the maximally entangled GHZ state.

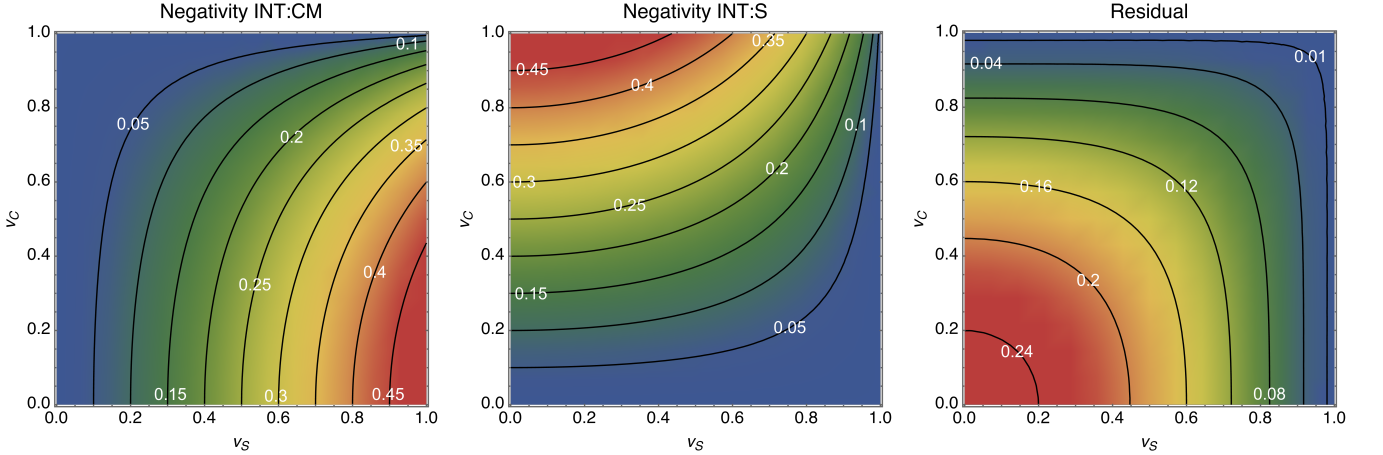


FIG. 8. Dependence of negativity on v_S and v_C for reduced bipartite states. Left panel: INT:CM. Middle panel: INT:S. Right panel: residual entanglement, which quantifies genuine tripartite entanglement. For the CG case, since $v_S = 1$, $\mathcal{N}(\rho_{\text{INT:S}})$ is always zero, but $\mathcal{N}(\rho_{\text{INT:CM}}) \neq 0$ depending on the value of v_C .

Finally, we evaluated the entanglement entropy in our system. In Fig. 9, we depicted the time dependence of the entanglement entropy between unipartite-bipartite systems. The left panel shows the CG case, and the right panel shows the QG case. The orange line shows CM:others systems, the blue line shows INT:others systems and the green line shows the S:others systems. Parameters are chosen as the same as in Fig. 6, namely $(m_0^3/k)^{1/2} = 10$, $(m_0/m_1)^{1/2} = 0.5$, $Gm_0M/(kd^3) = 0.015$, $m_0^{1/4}d = 10$, $\beta/d = 0.01$, $\sigma/d = 0.001$. We see any entanglement entropy is bounded by $\log 2$ (gray dashed line), which value involves the GHZ state. In the CG case, We can see that the entanglement entropy of S:others systems vanishes. This means that the source system is isolated from the particle system due to the classical interaction. The entanglement entropy of CM:others and INT:others systems take the same value since they both show the entanglement shared between the CM system and the INT system. In the QG case, we can see the entanglement is shared between the whole 3 systems. Especially, the entanglement entropy

of INT:others and S:others almost reach the maximum value $\log 2$ when the visibility is at the minimum in Fig. 6. This is because the INT system is represented by 2 qubits and the S state is approximately represented by 2 qubits which nearly reads to the maximally entangled state.

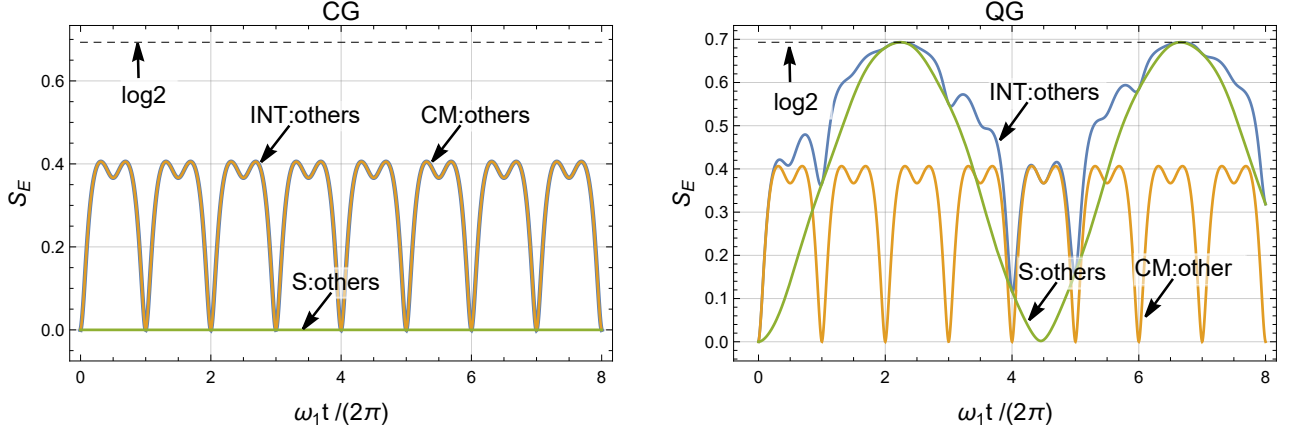


FIG. 9. Entanglement entropy between unipartite-bipartite systems for CG case (left panel) and QG case (right panel). Each line shows CM:others systems (orange line), INT:others systems (blue line), and S:others systems (green line). The gray dashed line shows $\log 2$; the maximally entangled state.

VI. DISCUSSION

In this section, we discuss the feasibility of detecting the quantumness of gravity in our proposal. Let us suppose an experiment being performed using an $^{27}\text{Al}^+$ quantum clock [30] with a probe laser wavelength $\lambda = 2\pi\hbar c/E = 267 \text{ nm}$. A coherent state of the mesoscopic mass source with $M \sim 1 \text{ ng}$ may be realized in the near future. In addition, the coherent state can be experimentally realized for 20 sec [31]. Apart from that, we assume $d = 200 \mu\text{m}$, $\sigma = 1 \mu\text{m}$ and $\beta = 10 \mu\text{m}$ to compare setups of the BMV proposal [9–11]. Therefore, for a duration of coherence time scale t , the fractional change of the decoherence factor in $|\mathcal{V}_Q(t)|$ of Eq. (48) can be estimated as

$$\left(\frac{1}{2\hbar} \frac{GME}{d} \frac{\sigma}{d} t\right)^2 = 1.7 \times 10^{-34} \left(\frac{M}{10 \text{ ng}}\right)^2 \left(\frac{\lambda}{267 \text{ nm}}\right)^{-2} \left(\frac{d}{200 \mu\text{m}}\right)^{-4} \left(\frac{\sigma}{1 \mu\text{m}}\right)^2 \left(\frac{t}{20 \text{ sec}}\right)^2, \quad (79)$$

$$\left(\frac{1}{\hbar} \frac{GME}{d} \frac{\beta}{d} t\right)^2 = 6.8 \times 10^{-32} \left(\frac{M}{10 \text{ ng}}\right)^2 \left(\frac{\lambda}{267 \text{ nm}}\right)^{-2} \left(\frac{d}{200 \mu\text{m}}\right)^{-4} \left(\frac{\beta}{10 \mu\text{m}}\right)^2 \left(\frac{t}{20 \text{ sec}}\right)^2. \quad (80)$$

After performing time Fourier transformation on the probability $P(t)$ obtained using the spectroscopy experiments, the least necessary precision to detect the QG effect in our proposal is approximately 10^{-32} , which is extremely small to be distinguished in the present clock spectroscopy, whose observation uncertainty is about 10^{-19} [30]. Let us discuss our result Eq. (80) in comparison with visibility change obtained by the setup of Carney *et al.* [19]. Carney *et al.* investigated entanglement between a massive oscillator and a source mass particle with a cat state, and evaluated the interference visibility of the particle state. Their estimation of the time change of the visibility due to quantum gravitational interaction is

$$\left(\frac{GMm}{d} \frac{\beta}{d} \frac{x_0}{d} t\right)^2 \propto d^{-6}, \quad (81)$$

where x_0 is the spread of the ground state wave function of the oscillator. For the optimal values of parameters in their setup, the ratio provides a value of $\sim 10^{-28}$. Although Eq. (80) exhibits a lower suppression factor d^2 compared to (81), the ratio E/m makes the visibility change smaller compared to that in Eq. (81).

As a crucial issue of this study, we also discuss the uniqueness of gravity compared to other quantum interactions, such as the electromagnetic Coulomb force. In our setup, CG creates an entanglement only between the CM and INT systems, whereas all subsystems share entanglement in the QG case. It should be noted that, in particular, the entanglement between the INT and S systems is uniquely induced by the quantumness of gravity, and no other quantum interactions can establish this entanglement. This is because according to the weak equivalence principle and the mass-energy equivalence, only gravity can couple to the energy; other quantum interactions do not have this

property [4]. Figure 10 depicts the entanglement structure for different external forces, namely CG, QG, and Coulomb force. To capture the uniqueness of the quantumness of gravity, we should detect entanglement held between the INT system and the S system.

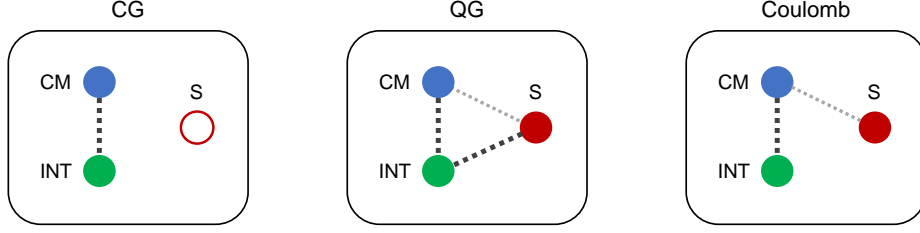


FIG. 10. Entanglement structure for the CG, QG, and Coulomb interaction cases. Dotted lines represent the existence of couplings between degrees of freedom, and possible pairs of subsystems sharing entanglement. For the QG case, the total system shares genuine tripartite entanglement which cannot be reduced to bipartite entanglement between the reduced bipartite systems. For the quantum Coulomb case, tripartite entanglement is reduced to bipartite entanglement between the reduced bipartite systems.

For comparison, let us consider the case when the Coulomb interaction is the external force instead of the gravitational interaction. To focus on the connection of mass-energy equivalence with entanglement here, we do not consider a dipole-photon interaction which introduces a direct coupling between the INT and S system.² The Coulomb interaction is given by

$$V_{\text{Coulomb}} = \frac{qQ}{4\pi\epsilon_0|d + \hat{X} - \hat{x}|}, \quad (82)$$

where q and Q are the electric charges of the oscillator and the source, respectively. In comparison with the QG interaction

$$V_{\text{QG}} = -\frac{G\hat{m}M}{|d + \hat{X} - \hat{x}|}, \quad (83)$$

the Coulomb interaction does not contain the INT operator \hat{m} as a result of the weak equivalence principle. Then, it is obvious that the Coulomb interaction does not produce the entanglement between the INT and S systems as depicted in Fig. 10. The Hamiltonian for the external Coulomb interaction can be expressed as

$$\hat{H}_{\text{Coulomb}}(\hat{X}) = \sum_{j=0,1} \left[\mathcal{E}_j(\hat{X}) + \frac{\hat{p}^2}{2m_j} + \frac{m_j\omega_j^2}{2} \left(\hat{x} - \frac{qB(\hat{X})}{k} \right)^2 \right] |E_j\rangle \langle E_j|, \quad \mathcal{E}_j(\hat{X}) = m_j - qA(\hat{X}) - \frac{q^2B^2(\hat{X})}{2k}, \quad (84)$$

$$A(\hat{X}) = \frac{Q}{4\pi\epsilon_0 d} \left(1 - \frac{\hat{X}}{d} + \frac{\hat{X}^2}{d^2} \right), \quad B(\hat{X}) = \frac{Q}{4\pi\epsilon_0 d^2} \left(1 - \frac{2\hat{X}}{d} \right), \quad C = \frac{Q}{4\pi\epsilon_0 d^3}. \quad (85)$$

Unlike the gravity case, the symmetry axis of the trapping potential is independent of the INT state, and the quantity $\mathcal{E}_1(\hat{X}) - \mathcal{E}_0(\hat{X})$ is independent of \hat{X} . As a result, the visibility of the Coulomb force case exhibits a different behavior compared to the CG and QG cases. Following the same procedure used to derive Eq. (50), we obtain the π/ω_1 periodic visibility as

$$|\langle \Psi_0(t) | \Psi_1(t) \rangle| = \left(\frac{4a_0 a_1}{4a_0 a_1 \cos^2(\omega_1 t) + (a_0 + a_1)^2 \sin^2(\omega_1 t)} \right)^{1/4}. \quad (86)$$

Here, the period $2\pi/\omega_1$ of coherent state does not appear since the displacement factor $\Delta(\hat{X}) := qB(\hat{X})/k \approx Q/d^2$ is independent of the internal energy level. Therefore, up to the leading order in Eq. (18), we conclude that the nonrevival

² Note that we have made an assumption in our setup that the internal degrees of freedom of the particle are labeled only by the energy levels, which results in the unique correspondence of the INT:S entanglement and QG. Generally, the internal degrees of freedom of an atom are labeled not only by energy level but also by spin. In such cases, the dipole-photon interaction can also create INT:S entanglement besides gravity. A general form of the dipole-photon interaction is given by $\hat{\mathbf{d}} \cdot \hat{\mathbf{E}}$, where $\hat{\mathbf{d}} = d_+ |E_1\rangle \langle E_0| + d_- |E_0\rangle \langle E_1|$ is the electric dipole moment operator of the INT system, and $\hat{\mathbf{E}}$ is the external electric field. When the external electric field has the source (S) dependence as $\hat{\mathbf{E}}(\hat{X})$, this interaction can provide the INT-S entanglement in the leading order of expansion for the source separation.

behavior in visibility uniquely discriminates the quantumness of gravity. The visibility is more likely to exhibit revival behavior for the Coulomb interaction case than the QG case since the former shares less entanglement than the latter, as in Fig. 10. The left panel of Fig. 11 presents the behavior of the probability for the Coulomb interaction by evaluating up to the second-order of Taylor expansion in Eq. (18). The parameters are set to $(m_0^3/k)^{1/2} = 10$, $(m_0/m_1)^{1/2} = 0.85$, $qQ/(4\pi\epsilon_0kd^3) = 0.15$, $m_0^{1/4}d = 10$, $\beta/d = 0.01$, $\sigma/d = 0.001$. As the figure shows, the visibility exhibits a revival behavior with some longer period than π/ω_1 obtained by the first-order approximation in Eq. (86). This is because the visibility beats due to the addition of two functions with periods $2\pi/\omega_0$ and $2\pi/\omega_1$, reflecting the respective period of the coherent states $|\Psi_0(t)\rangle$ and $|\Psi_1(t)\rangle$ as an effect of the external quantum Coulomb force. In the first-order approximation, the displacement effects of these coherent states are neglected. Regarding the behavior of negativity, within the first order approximation, $v_S = 1$ results in $\mathcal{N}(\rho_{\text{INT:S}}) = 0$ and provides a nonzero value of $\mathcal{N}(\rho_{\text{CM:INT}})$ with period π/ω_1 . The quantumness of Coulomb force appears as a small nonzero value of $\mathcal{N}_{\text{CM:S}}$, which can be revealed beyond the first-order approximation, as per the right panel of Fig. 11.

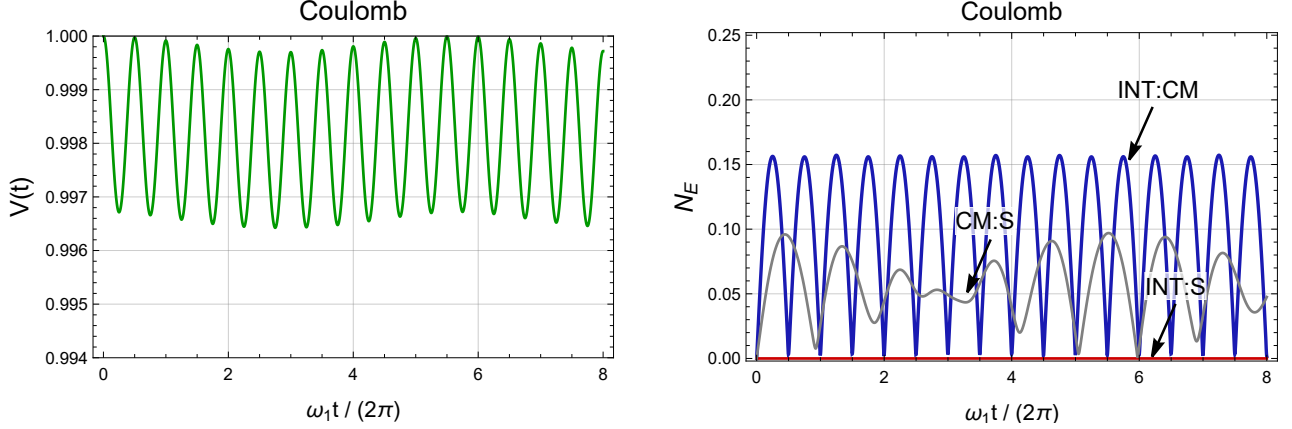


FIG. 11. Left panel: time dependence of the visibility $\mathcal{V}(t)$ for the Coulomb case. Right panel: logarithmic negativity for the Coulomb case; Red line: bipartite INT:S subsystems. Blue line: bipartite INT:CM subsystem. Grayline: bipartite CM:S subsystem.

Also, we briefly discuss the case where the harmonic oscillator potential trapping the particle is proportional to the probe mass [32]: $\frac{1}{2}\hat{m}\omega^2\hat{x}^2$, where ω is a constant parameter. Here, a shift of the potential due to the external gravity becomes independent of the internal energy level, and we obtain $\Delta_1 = \Delta_0 \neq 0$. Since the displacement effect does not become obvious in the Ramsey interference, $|\mathcal{V}_C(t)|$ reduces to a π/ω_1 periodic function rather than $2\pi/\omega_1$ periodic function. Therefore, the visibility revival period becomes π/ω_1 for the CG case, while it does not exhibit revival for the QG case due to the quantumness of gravity.

Finally, we comment on the relevance of the alternative theories of gravity. Since our proposal are focusing only on the nonrelativistic scale, it is difficult to distinguish alternative theories of gravity when they reduce to the Newtonian gravity in the Newtonian limit. To distinguish them, we need experiment on the higher orders of $1/c^2$ expansion where the difference between alternative theories appears. It may be interesting to discuss how the Ramsey interference differs depending on alternative theories of gravity by analyzing the higher-order expansions, although the detection is technically difficult at present.

VII. SUMMARY

In this study, we investigated the quantumness of gravity in the setup of the Ramsey interferometry. For the classical external gravitational field, the interference visibility exhibits oscillatory behavior, and the coherence between the two energy states exhibits collapse and revival behavior in time. The decoherence behavior originated from the coupling between the CM state and INT state due to the mass-energy equivalence principle. On the other hand, when a gravitational source is in quantum superposition, the visibility exhibited additional oscillation with a longer period and decay at a long time scale for the QG case, while it remains $2\pi/\omega_1$ periodic in the CG case. For the zero spread of the source state, the time scale of decoherence was determined as $t \sim \left(\frac{GME}{d} \frac{\beta}{d}\right)^{-1}$, which constrains the feasibility of the experimental detection of the quantumness of gravity. In addition, we found that the spread of the source

wave function provides another decoherence effect that is not periodic in time depending on the variance of the source Gaussian state σ .

Regarding the entanglement behavior, the initial separable CM-INT-S system acquired genuine tripartite entanglement due to the quantumness of gravity. On the contrary, the quantumness of the Coulomb force cannot acquire the entanglement between the INT and S systems. This is because the Coulomb interaction does not couple to mass-energy of the INT state, unlike gravity, which obeys the weak equivalence principle. Since the nonrevival feature of the interference visibility reproduce the entanglement between the INT and S systems, it is possible to distinguish the quantumness of gravity from other quantum interactions by observing the visibility of Ramsey interference. We believe that our study is beneficial for further understanding of the quantum nature of gravity.

ACKNOWLEDGMENTS

We would like to thank A. Matsumura and K. Yamamoto for providing their valuable insight on the subject. This research was supported in part by the Japan Science and Technology Agency (JST), the Nagoya University Interdisciplinary Frontier Fellowship (Y.K.), and JSPS KAKENHI Grant No. 19K03866 (Y.N.) and No. 22H05257 (Y.N.).

Appendix A: WIGNER FUNCTION OF TIME EVOLVED CM STATE

In this section we will investigate the time evolution of the CM state $|\psi_{j,X}(t)\rangle$ by depicting its Wigner function [33], which gives us an intuitive understanding of the visibility behavior.

In the QG case, the time-evolved CM state is given by

$$|\psi_{j,X}(t)\rangle = \hat{U}_{j,X}(t) |\psi_{\text{ini}}\rangle, \quad (\text{A1})$$

where $\hat{U}_{j,X}(t) := e^{-i\omega_j(\hat{a}_{j,X}^\dagger \hat{a}_{j,X} + 1/2)t}$, $|\psi_{\text{ini}}\rangle$ is the ground state of the Hamiltonian $\omega_j(\hat{a}_{0,0}^\dagger \hat{a}_{0,0} + 1/2)$, and $\hat{a}_{j,X}$ is as per Eq. (27). The relation between the two annihilation operators $\hat{a}_{0,0}$ and $\hat{a}_{j,X}$ is as follows, by

$$\hat{a}_{j,X} = \cosh r_j \hat{a}_{0,0} + \sinh r_j \hat{a}_{0,0}^\dagger + \alpha_{j,X}, \quad (\text{A2})$$

$$e^{r_j} = \sqrt{\frac{m_j \omega_j}{m_0 \omega_0}}, \quad \alpha_{j,X} = \sqrt{\frac{m_0 \omega_0}{2}} e^{r_j} (\Delta_0(0) - \Delta_j(X)). \quad (\text{A3})$$

Using the squeezing operator $\hat{S}(r_j) = e^{r_j(\hat{a}_{0,0}^2 - \hat{a}_{0,0}^{\dagger 2})/2}$ and the displacement operator $\hat{D}(\alpha) = e^{\alpha(\hat{a}_{0,0}^\dagger - \hat{a}_{0,0})}$, the relation of the two annihilation operators can be rewritten as

$$\hat{a}_{j,X} = \hat{S}^\dagger(r_j) \hat{D}^\dagger(\alpha_{j,X}) \hat{a}_{0,0} \hat{D}(\alpha_{j,X}) \hat{S}(r_j). \quad (\text{A4})$$

Therefore, the initial ground state $|\psi_{\text{ini}}(t)\rangle$ associated with $\hat{a}_{0,0}$ evolves to become the squeezed coherent state characterized by parameters r_j and $\alpha_{j,X}$ as given below,

$$|\psi_{j,X}(t)\rangle = \hat{S}^\dagger(r_j) \hat{D}^\dagger(\alpha_{j,X}) \hat{U}_{0,0} \hat{D}(\alpha_{j,X}) \hat{S}(r_j) |\psi_{\text{ini}}\rangle. \quad (\text{A5})$$

For the no gravity case, the time-evolved CM state is obtained by replacing $\alpha_{j,X} \rightarrow 0$. For the CG case, the time-evolved CM state is obtained by replacing $\alpha_{j,X} \rightarrow \alpha_j$.

Next, we explore the temporal behavior of the CM Wigner function [33]. The Wigner function is a quasiprobability distribution in the phase space (x, p) and is defined as

$$W_\psi(x, p) = \frac{1}{2\pi} \int_{-\infty}^{\infty} d\xi \psi\left(x + \frac{\xi}{2}\right) \psi^*\left(x - \frac{\xi}{2}\right) e^{i\xi p}, \quad (\text{A6})$$

where $\psi(x)$ is the wave function of the CM system. For simplicity, we focus on the state with $X = \pm\beta$, which is the same condition as we depicted in Fig. 4. Length unit of $2m_0\omega_0 = 1$.

Figure 12 displays the time evolution of the Wigner function of the CM state for the no gravity case. The blue and red regions respectively denote the Wigner function of the $|\psi_0(t)\rangle$ and $|\psi_1(t)\rangle$ states. The parameters are set to $e^{r_1} = 1.2$, $\omega_1/\omega_0 = 0.8$. Since there is no displacement effect due to gravity, the time-evolved state is simply squeezed due to a special relativistic effect. The two states overlap for every π/ω_1 period, which reflects the period of squeezing.

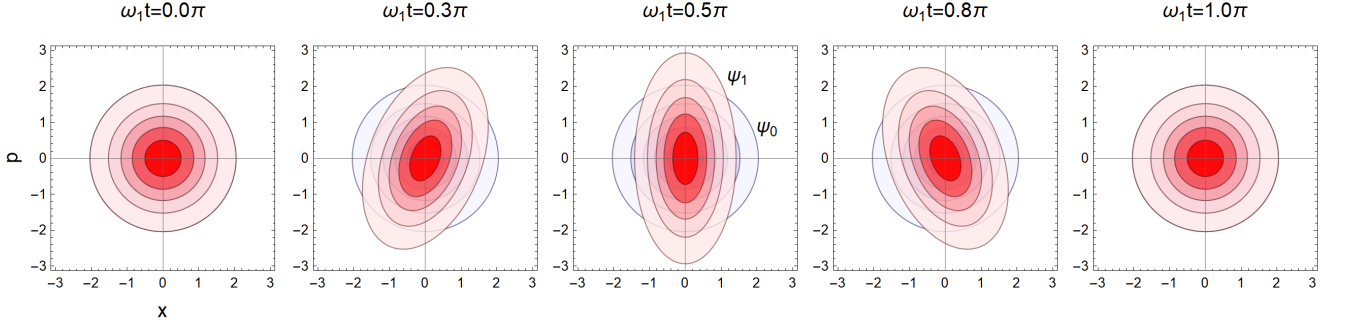


FIG. 12. Time evolution of the Wigner function of the CM state for the no gravity case. A blue region: Wigner function of the $|\psi_0(t)\rangle$ state. A red region: Wigner function of the $|\psi_1(t)\rangle$ state. Contour lines are drawn with (0.02, 0.05, 0.08, 0.11, 0.14).

Since the visibility of the Ramsey interference in Eq. (40) contains $|\langle\psi_0(t)|\psi_1(t)\rangle|$, its revival period π/ω_1 stems from the squeezing period.

Figure 13 displays the time evolution of the Wigner function of the CM state for the CG case. The blue and red regions respectively denote the Wigner function of $|\psi_0(t)\rangle$ and $|\psi_1(t)\rangle$ states. The parameters are set to $e^{r_1} = 1.2$, $\alpha_1 = 3$, $\omega_1/\omega_0 = 0.8$. The time evolved state is squeezed by a special relativistic effect and displaced by a gravitational effect. The two states overlap for every $2\pi/\omega_1$ period reflecting the period of coherent state, which results in the $2\pi/\omega_1$ revival period of the visibility.

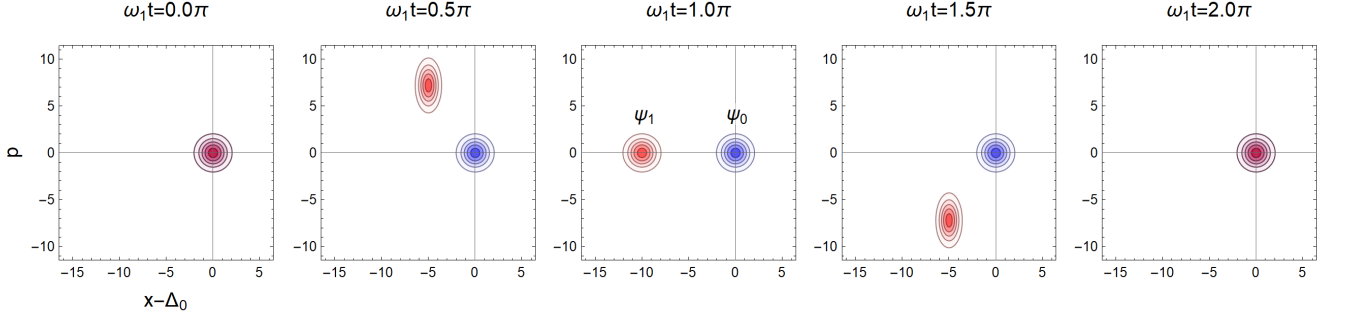


FIG. 13. Time evolution of the Wigner function of the CM state for the CG case. A blue region: Wigner function of the $|\psi_0(t)\rangle$ state. A red region: Wigner function of the $|\psi_1(t)\rangle$ state. Contour lines are drawn with (0.02, 0.05, 0.08, 0.11, 0.14).

Figure 14 displays the time evolution of the Wigner function of the CM state for the CG case. The blue region with solid contours denotes the Wigner function of $|\psi_{0,-\beta}(t)\rangle$, the blue region with dashed contours denotes the Wigner function of $|\psi_{0,+\beta}(t)\rangle$, the red region with solid contours denotes the Wigner function of $|\psi_{1,-\beta}(t)\rangle$, and the red region with dashed contours denotes the Wigner function of $|\psi_{1,+\beta}(t)\rangle$. The parameters are set to $e^{r_1} = 1.2$, $\alpha_{0,0} = 1.5$, $\alpha_{1,0} = 3.0$, $\alpha_{j,+\beta}/\alpha_{j,-\beta} = 0.6$, $\omega_1/\omega_0 = 0.8$. There are four kinds of squeezed-coherent states with $j = 0, 1$ and $X = \pm\beta$. The Wigner functions of $|\psi_{0,X}(t)\rangle$ and $|\psi_{1,X}(t)\rangle$ moves with different the time periods $2\pi/\omega_0$ and $2\pi/\omega_1$, respectively, and typically do not coincide. The nonrevival behavior of the visibility for the QG case is originated from the fact that these four states do not coincide, as well as the phase difference $e^{-i\mathcal{E}_{j,X}t}$ in Eq. (40).

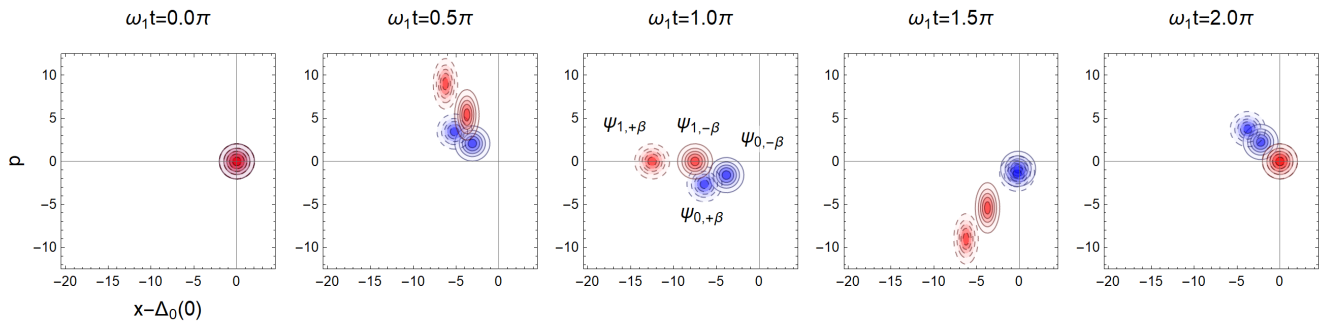


FIG. 14. Time evolution of the Wigner function of the CM state for the QG case. Blue region with solid contours: Wigner function of $|\psi_{0,-\beta}(t)\rangle$. Blue region with dashed contours: Wigner function of $|\psi_{0,+\beta}(t)\rangle$. Red region with solid contours: Wigner function of $|\psi_{1,-\beta}(t)\rangle$. Red region with dashed contours: Wigner function of $|\psi_{1,+\beta}(t)\rangle$. Contour lines are drawn with (0.02, 0.05, 0.08, 0.11, 0.14).

-
- [1] J. J. Sakurai, *Modern Quantum Mechanics* (Addison-Wesley, New York, 2011).
- [2] R. Colella, A. W. Overhauser, and S. A. Werner, Observation of Gravitationally Induced Quantum Interference, *Phys. Rev. Lett.* **34**, 1472 (1975).
- [3] H. Rauch and S. A. Werner, *Neutron Interferometry* (Oxford University Press, New York, 2000).
- [4] I. Pikovski, M. Zych, F. Costa, and C. Brukner, Universal decoherence due to gravitational time dilation, *Nat. Phys.* **11**, 668 (2015).
- [5] T. Bothwell, C. J. Kennedy, A. Aeppli, D. Kedar, J. M. Robinson, E. Oelker, A. Staron, and J. Ye, Resolving the gravitational redshift across a millimetre-scale atomic sample, *Nature (London)* **602**, 420 (2022).
- [6] M. Zych, I. Pikovski, F. Costa, and C. Brukner, General relativistic effects in quantum interference of “clocks”, *J. Phys. Conf. Ser.* **723**, 012044 (2016).
- [7] M. Zych, L. Rudnicki, and I. Pikovski, Gravitational mass of composite systems, *Phys. Rev. D* **99**, 104029 (2019).
- [8] R. Haustein, G. J. Milburn, and M. Zych, Mass-energy equivalence in harmonically trapped particles, [arXiv:1906.03980](https://arxiv.org/abs/1906.03980).
- [9] S. Bose, A. Mazumdar, G. W. Morley, H. Ulbricht, M. Toroš, M. Paternostro, A. Geraci, P. Barker, M. S. Kim, and G. Milburn, A Spin Entanglement Witness for Quantum Gravity, *Phys. Rev. Lett.* **119**, 240401 (2017).
- [10] C. Marletto and V. Vedral, Gravitationally Induced Entanglement between Two Massive Particles is Sufficient Evidence of Quantum Effects in Gravity, *Phys. Rev. Lett.* **119**, 240402 (2017).
- [11] M. Christodoulou and C. Rovelli, On the possibility of laboratory evidence for quantum superposition of geometries, *Phys. Lett. B* **792**, 64 (2019).
- [12] M. A. Nielsen and I. L. Chuang, *Quantum Computation and Quantum Information* (Cambridge University Press, Cambridge, England, 2000).
- [13] D. Carney, P. C. Stamp, and J. M. Taylor, Tabletop experiments for quantum gravity: A user’s manual, *Classical Quantum Gravity* **36**, 034001 (2019).
- [14] A. Matsumura and K. Yamamoto, Gravity-induced entanglement in optomechanical systems, *Phys. Rev. D* **102**, 106021 (2020).
- [15] A. Matsumura, Y. Nambu, and K. Yamamoto, Leggett-Garg inequalities for testing quantumness of gravity, *Phys. Rev. A* **106**, 012214 (2022).
- [16] R. Feynman and F. Vernon, The theory of a general quantum system interacting with a linear dissipative system, *Ann. Phys. (N.Y.)* **281**, 547 (2000).
- [17] E. Joos and H. D. Zeh, The emergence of classical properties through interaction with the environment, *Z. Phys. B Condens. Matter* **59**, 223 (1985).
- [18] W. H. Zurek, Decoherence, einselection, and the quantum origins of the classical, *Rev. Mod. Phys.* **75**, 715 (2003).
- [19] D. Carney, H. Müller, and J. M. Taylor, Using an atom interferometer to infer gravitational entanglement generation, *PRX Quantum* **2**, 030330 (2021).
- [20] K. Streltsov, J. S. Pedernales, and M. B. Plenio, On the significance of interferometric revivals for the fundamental description of gravity, *Universe* **8**, 58 (2022).
- [21] T. Kibble, Relativistic models of nonlinear quantum mechanics, *Commun. Math. Phys.* **64**, 73 (1978).
- [22] T. W. B. Kibble and S. Randjbar-Daemi, Non-linear coupling of quantum theory and classical gravity, *J. Phys. A* **13**, 141 (1980).
- [23] L. Diósi, Gravitation and quantum-mechanical localization of macro-objects, *Phys. Lett. A* **105**, 199 (1984).
- [24] N. F. Ramsey, A molecular beam resonance method with separated oscillating fields, *Phys. Rev.* **78**, 695 (1950).

- [25] A. D. Cronin, J. Schmiedmayer, and D. E. Pritchard, Optics and interferometry with atoms and molecules, *Rev. Mod. Phys.* **81**, 1051 (2009).
- [26] S. Abend, M. Gersemann, C. Schubert, D. Schlippert, E. M. Rasel, M. Zimmermann, M. A. Efremov, A. Roura, F. A. Narducci, and W. P. Schleich, Atom interferometry and its applications, *Proc. Int. Sch. Phys. "Enrico Fermi"* **197**, 345 (2020).
- [27] H. A. Gersch, Time evolution of minimum uncertainty states of a harmonic oscillator, *Am. J. Phys.* **60**, 1024 (1992).
- [28] G. Vidal and R. Werner, Computable measure of entanglement, *Phys. Rev. A* **65**, 032314 (2002).
- [29] Y.-C. Ou and H. Fan, Monogamy inequality in terms of negativity for three-qubit states, *Phys. Rev. A* **75**, 062308 (2007).
- [30] S. M. Brewer, J.-S. Chen, A. M. Hankin, E. R. Clements, C. W. Chou, D. J. Wineland, D. B. Hume, and D. R. Leibrandt, $^{27}\text{Al}^+$ Quantum-Logic Clock with a Systematic Uncertainty Below 10^{-18} , *Phys. Rev. Lett.* **123**, 033201 (2019).
- [31] V. Xu, M. Jaffe, C. D. Panda, S. L. Kristensen, L. W. Clark, and H. Müller, Probing gravity by holding atoms for 20 seconds, *Science* **366**, 745 (2019).
- [32] H. Katori, Optical lattice clocks and quantum metrology, *Nat. Photonics* **5**, 203 (2011).
- [33] E. Wigner, On the quantum correction for thermodynamic equilibrium, *Phys. Rev.* **40**, 749 (1932).